DETERMINATION OF THE OPTIMUM WORKING CONDITIONS

OF A

DOUBLE RESONANCE SPECTROMETER

BY

CHANNAPPA KUKKUWADA. H

A Thesis submitted to the faculty of
Graduate Studies and Research in the
Partial fulfilment of the requirements
for the degree of Master of Science

The Eaton Electronics Research Laboratory
McGill University
Montreal

August 1963

TABLE OF CONTENTS

TABLE OF CONTENTS
(Continued)

ACKNOWLEDGEMENTS

This work was done under the supervision of Dr. D.J.I.Fry to whom the author wishes to express his appreciation and sincere thanks for his consistent guidance and valuable discussions. Grateful thanks are also due to Professor G.A.Woonton, Chairman of the Department, for many stimulating discussions and for providing grants during the summers of 1962 and 1963.

Thanks are also due to Mr. V. Avarlaid, and his staff for their timely co-operation in making possible this work.

Members of the staff and graduate students of the Eaton Laboratory must be thanked for many helpful discussions the author had with them.

Mr. P. W. Smith provided the crystals used for this project made by Hansler. The author appreciates his help. The initial part of this work was done with the collaboration of Mr. Armen Manoogian. The author wishes to thank him for his co-operation.

ABSTRACT

The subject of this thesis is the work done in the Eaton Electronics Research Laboratory as a beginning of a programme of studies of double resonance.

The aim of this work is to find out the conditions under which the best ENDOR signal can be obtained. A reflection cavity was used for all the results described, since the original transmission cavity developed faults.

The samples used were crystals of magnesium oxide containing small amounts of cobalt impurity, present as Co^{++} ions. Co^{++} ions in MgO are known to be in surroundings of accurately cubic symmetry. Samples of 5%, 2% and 0.5% nominal concentrations were used and for each concentration, conditions for the best ENDOR signal were found and are reported. The basic spectrometer is similar in principle to that used by Feher[15] for electron paramagnetic resonance measurements except that the necessary additional equipment was added for double resonance.

The dependence of ENDOR signal on amount of F.M., A.M. and γ_Q - voltage was linear, as expected, with however

evidence of departures from linearity in the case of the γ_2 - graph. The variation of ENDOR signal with microwave power showed a fairly sharp maximum, at a power dependent on the concentration of Co^{++} ions in the sample. A simple theory predicts a maximum when the spin temperature is doubled, and was supported by the results. F.M. was found to be preferable to A.M. for the samples used.

I. 1. INTRODUCTION

As the name "ENDOR" -(Electron-Nuclear double resonance or simply "Double Resonance" as it is frequently called) - itself suggests , both electronic and nuclear transitions are involved. This technique requires partial saturation of the electron paramagnetic resonance (EPR) signal under investigation. The double resonance method has been extended by Feher[1] to observe nuclear transitions and thereby determine hyperfine interactions and nuclear g-factors.

The object of this work is to set up an ENDOR spectrometer and evaluate its performance. Several methods are available for achieving production and detection of the signal, and so a comparison of these is desirable. The optimum conditions are of course rather important, and also interesting on their own account, as they should throw some light on the rather complicated processes involved in double resonance.

The phenomenon of electron paramagnetic resonance is quite well-known as a method for studying dilute paramagnetic substances. The permanent magnetic dipoles change their orientations with respect to an applied steady magnetic field when an oscillating magnetic field of appropriate radio frequency is applied.

In the case of an ion which also possesses a nuclear spin, the energy level scheme is complicated by the fact that

each electron orientation level is subdivided into close-spaced levels corresponding to the different orientations of the nuclear spin. The spectrum of absorption as a function of magnetic field is invariably changed, each electron resonance line splitting into several close lines because of the nuclear spin. ENDOR is a method of measuring the spacing of the close lines directly, by inducing direct transitions between the components of an electron line split by nuclear spin, at the same time as the electronic transitions are being induced, by applying a second radio frequency oscillating field, of rather lower frequency. It is experimentally more convenient to detect the small energy nuclear transitions by means of their effect on the higher energy electronic transitions, requiring two different frequencies and so the name double resonance is appropriate.

As paramagnetic resonance experiments are inevitable in the course of study of double resonance experiments, it seems necessary to give the theory, in brief, of paramagnetic resonance before going further into the field of double resonance, which is, in effect, a development of the former.

2. Paramagnetic Resonance:-

Even though the aim of this work is to study the optimum conditions for observing a double resonance transition, in order to understand double resonance it is necessary to

understand the mechanism of paramagnetic resonance as the nature of ENDOR lines depends upon those of the EPR lines. A brief discussion of this is given here. For a full and detailed discussion of this subject reference should be made to various review articles in general and to those by Bleaney and Stevens,[2] Bowers and Owen[3] in particular.

Magnetic resonance forms the basis of a branch of spectroscopy which has been a valuable addition to the methods of investigating the solid state. Under this heading we can also add the "Electron-Nuclear double resonance" in addition to nuclear resonance, paramagnetic resonance (EPR), ferromagnetic resonance and antiferromagnetic resonance. With the exception of only the nuclear resonance which is concerned with nuclear dipoles all the rest are concerned with electronic dipoles. Paramagnetic resonance deals with magnetic systems where the electronic dipoles are loosely coupled systems where the paramagnetic units may be regarded as individuals.

The present work deals with the study of paramagnetism, i.e. the magnetic properties of substances, in which each permanent magnetic dipole is substantially independent of its neighbours. The theory then treats each dipole separately, and the effects of the neighbouring dipoles enter only in a subsidiary manner. Quantum theory gives a natural explanation of the presence of permanent magnetic dipoles. According to

this theory permanent dipoles occur whenever the atom or the ion contains partly filled electron shells. Such systems have resultant angular momentum due partly to the orbital motion and partly to the intrinsic spin of the electrons, with each of which is associated a magnetic dipole moment. The requirement of a partly filled electron shell in order that it may possess permanent magnetic dipoles therefore restricts the occurrence of paramagnetism in compounds of certain well-defined regions of the periodic table, known as transition groups. Of these transition-groups the most fully investigated is the iron-group with the 3d-shell being partly filled.

Most of the paramagnetic substances are solids. In the iron-group, with which this work is concerned, the magnetic susceptibility was found to be much closer to that which would be expected from the electron spins alone than that calculated for an agglomeration of free ions. The reason for this was found to be the strong interaction between the paramagnetic ion and its immediate surroundings, the diamagnetic material, in which it is imbedded. These diamagnetic neighbours are charged and hence produce a strong electrostatic field, through which the electrons of the paramagnetic ion must move.

The effect of the electric field may be quite strong

so that the coupling between the orbital angular momentum vector L and spin angular momentum vector S, with the allowed values M_L and M_S respectively, in the direction of the applied field is broken as a result of which each precesses about the direction of the electric field separately. Then J, the vector sum of L and S, no longer has any meaning. The quantum numbers to be used for different energy levels are M_L and M_S. M_S has the values S, S-1, ...to -S, which is $2S + 1$ values in all. Usually, the splitting produced between different M_L levels by such a field is of the order of 10^3 cm^{-1} and hence only the lowest level is populated at ordinary temperatures thus "Quenching" the orbital momentum. In the iron-group,electrons are fully exposed to the field of the neighbours, and the effect of the crystalline electric field is so great that the orbital motion is "quenched". This means that the orbital motion is "locked into" the field of the neighbours, and is unable to make its proper contribution to the magnetism. The electron spin, however, with its corresponding magnetic moment, has no direct interaction with the crystalline electric field, and hence remains free to orient itself in an external magnetic field. Thus the magnetic properties of the salts of the iron-group correspond to "spin-only" magnetism.

II. 1. RESONANCE CONDITION

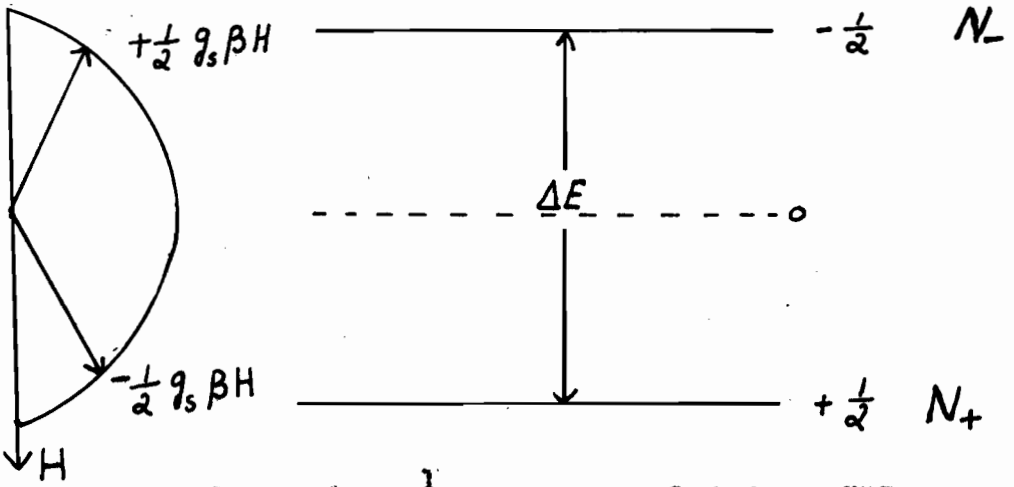

Fig. 1. A Spin $\frac{1}{2}$ system explaining EPR.

The phenomenon of paramagnetic resonance is shown in its simplest form by a set of non-interacting paramagnetic ions, each possessing a single unpaired electron and a magnetic dipole moment of $\frac{1}{2} g_s \beta$, where $\beta = eh/4\pi mc$, is the Bohr magneton, and g_s is spectroscopic splitting factor. In a steady magnetic field H, each dipole can orient itself parallel to H with the energy $-\frac{1}{2} g_s \beta H$ or anti-parallel to it with the energy $+\frac{1}{2} g_s \beta H$ as represented diagrammatically above. These two possible energy levels are separated by a gap of $\Delta E = g_s \beta H$. If we now apply radiation of the resonant frequency ν_1 polarized in a direction perpendicular to the steady magnetic field H, such that

$$h\nu_1 = \hbar\omega_1 = g_s \beta H \qquad \text{- - - - - - (1)}$$

is the energy of each quantum, transitions between the levels obeying the selection rules $\Delta M_s = \pm 1$ are induced. We know

from the theory of the Einstein coefficients, that the probability of transitions upwards by absorption is equal to the probability of transitions downwards by stimulated emission. In comparison with these probabilities, the probability of transitions downwards by spontaneous emission is quite negligible. If the populations of the energy levels were equal, the average rate of transitions up and down would therefore be equal, and there would be no net effect on the system. Actually, however, since the spins are in equilibrium at temperature T_s, the population of the lower level exceeds that of the upper level by the Boltzman factor

$$\exp {}^{\Delta E}/_{KT_s},$$ where K is the Boltzman constant

T_s is the spin temperature

On account of this excess of population in the lower energy state, there is a net absorption of energy from the microwave field.

In order to induce magnetic dipole transitions between these two energy levels we must apply a high frequency magnetic field of frequency ν_1 such that the quantum of high frequency energy equals the separation between the levels according to equation (1). Thus there is resonance absorption corresponding to the dipoles being flipped from the parallel to the anti-parallel state and there is induced

emission corresponding to the reverse process.

If the system remains in thermal equilibrium, more spins are in the parallel state because it is of lower energy, so that there is a net absorption of microwave power. In the actual paramagnetic resonance experiments this absorption can be measured by placing the sample in a cavity resonator, and detecting the drop in the transmitted microwave power at resonance. The normal practice of experimenting is to keep the frequency fixed and to vary the field H so that, for the example discussed above, if H is steadily increased a single absorption line is found at the H value given by $H = \frac{h\nu_l}{g_s\beta}$.

In principle the radiation requires to be circularly polorized, but in practice linearly polorized radiation is sufficient, since an oscillating field can be considered as two fields of half the amplitude rotating in opposite directions.

Let us now suppose that there is a large number N of electrons. Following the same treatment as that given by Andrew[4] for an assembly of Nuclei, let N_- electrons occupy the upper energy state, and N_+ electrons occupy the lower energy state. Let W_- be the probability per unit time for downward transitions and W_+ be the probability per unit

time for upward transitions. If the whole system of spins and lattice is in thermal equilibrium at a temperature T, then by the principle of detailed balancing, the number of transitions upwards and downwards must be equal. Hence

$$W_- N_- = W_+ N_+ \qquad \text{-------(2)}$$

But $\frac{N_+}{N_-} = \exp \frac{\Delta E}{KT}$ By the Boltzmann's Distribution

$$\cong 1 + \frac{\Delta E}{KT} \qquad \text{-------(3)}$$

Hence $W_- = W \left(1 + \frac{\Delta E}{2\ KT} \right)$ -------(4)

And $W_+ = W \left(1 - \frac{\Delta E}{2\ KT} \right)$

Where $W = \frac{W_- + W_+}{2}$

The above picture changes if we now consider that the spin system is at a different temperature T_s from that of the lattice which we assume to be at T. The excess number of spins n in the lower state is then given by

$$n = N_+ - N_- \qquad \text{-------(5)}$$

For each transition this excess changes by 2. Therefore the rate of change of n is given by

$$\frac{dn}{dt} = 2\ N_- W_- - 2\ N_+ W_+ \qquad \text{-------(6)}$$

$$= 2W\left\{N_-\left(1+\frac{\Delta E}{2KT}\right)\right\} - 2W\left\{N_+\left(1-\frac{\Delta E}{2KT}\right)\right\}$$

$$= 2W\ (n_o - n) \qquad \text{----(7)}$$

Where

$$n_o = (N_- + N_+)\ \frac{\Delta E}{2KT} = \frac{N\Delta E}{2\ KT} \qquad \text{----(8)}$$

Where

$N = N_- + N_+$ is the total number of spins

Thus n_o is the value of n when the spin system is in thermal equilibrium with the lattice. If (7) is integrated, we get

$$(n_o - n) = (n_o - n_i)\, e^{-2Wt} \qquad \text{----(9)}$$

Where n_i is the initial value of n. From the above equation we see that equilibrium is reached exponentially with a characteristic time $T_1 = 1/2\ W$ ----(10) which is called spin-lattice relaxation time. The spin-lattice relaxation time whose typical value encountered experimentally ranges from 10^{-12} to 10^{4} seconds has negligible effect on the line-width in comparison with other sources. The relaxation time depends upon the temperature, becoming longer at low temperatures. Also T_1 depends very markedly on the separation between the ground state and the first excited state - large T_1 for large separation and short T_1 for small separation.

In addition to the spin-lattice interaction there is another type of interaction taking place in the paramagnetic sample, due to the interaction between the spins themselves. Being magnetic dipoles, they produce a small magnetic field at the neighbouring dipoles. The result of this is that any paramagnetic ion will be subjected to the field of the remaining ions in the sample. But by Van Vleck's[5] Q.M. work this field, at a given ion, due to others in the sample is inversely proportional to the cube of the distance between the two ions. Hence the effect of only the nearest neighbours need taken into account. As with all interactions of this sort, it depends on the angle between the spins and on the angle between the spin and the vector to the other ion. Each ion is regarded as precessing about the external field, and its effect can be resolved into two components:

(a) A steady component directed along the field. This sets up a steady field at any other ion as a result of which this ion is situated in a field whose intensity is slightly different from the applied field. This process gives a broadening which is similar to that arising from an inhomogeneous field.

(b) The second component is a rotating component acting at right angles to the D.C. field, setting up a rotating field. If the frequency of the rotating field is equal to

the precessional frequency of any other ion there will be a couple acting on this second magnetic ion tending to change its direction. This component gives a resonance broadening, in the same way as for spin-lattice relaxation, because it tends to reduce the lifetime of an ion in a given state.

The broadening due to the steady component and rotating component is found to be independent of the temperature, though it has strong dependence on the concentration of the paramagnetic sample. The more concentrated the crystal is, the wider the line obtained.

2. Saturation:-

Having considered the rate at which the spin system and the lattice approach thermal equilibrium, we will now study its condition when it has settled down to a steady state under the influence of radiation. If it were not due to spin-lattice relaxation, the populations of the levels would be equalized. If a strong microwave field is applied, transitions may be induced by radiation. These transition rates may be comparable with transitions by relaxation processes, and as a result the original thermal equilibrium conditions will be destroyed. As the microwave field is increased, the population of the upper level increases and eventually a new dynamic equilibrium is attained. The ratio of the lower to the upper population for a two level system

considered before is given by equation (3) at thermal equilibrium. In the absence of radiation, the time variation of the excess number of spins following equations (7) and (10) is given by

$$\frac{dn}{dt} = \frac{n_o - n}{T_1} \qquad \text{- - - - - - - - -(11)}$$

In the presence of radiation, we have

$$\frac{dn}{dt} = \frac{n_o - n}{T_1} - 2np \qquad \text{- - - - - (12)}$$

Where P is the probability per unit time of a transition being induced between the levels under the influence of radiation. In the steady state, the time variation of the excess n must vanish. If n_s is the steady state value of this excess, then we have

$$\frac{n_s}{n_o} = \frac{1}{1 + 2PT_1} \qquad \text{- - - - - - - - -(13)}$$

But for a two level system we have, [4]

$$P = \frac{1}{4}\gamma^2 H_1^2 \, g(\nu)_{max.}$$

But $T_2 = \frac{1}{2} g(\nu)_{max.}$

$$\therefore P = \frac{1}{2}\gamma^2 H_1^2 T_2 \qquad \text{- - - - - - - - - (14)}$$

And $n_s / n_o = \left[1 + \frac{1}{2}\gamma^2 H_1^2 T_1 g(\nu)\right]^{-1} \equiv Z \qquad \text{- - - -(15)}$

Where T_2 is the spin - spin relaxation time

$g(\nu)$ is the normalized shape function and

γ is the electronic g - factor

Z is called the saturation factor.

If N_+^1 and N_-^1 are the new equilibrium populations of the lower and upper levels respectively, then we have

$$\frac{N_+^1}{N_-^1} = \exp \frac{\Delta E}{KT_s}$$

Where T_s is the new temperature of the spin system which is greater than the lattice temperature, consistent with a net absorption of energy. This indicates that the difference in population between the two levels has been reduced. But the absorption signal is directly proportional to the excess number of spins which, in turn, is inversely proportional to the temperature. Hence the absorption signal now becomes smaller. This phenomenon is known as saturation. The absorption signal increases with microwave power initially because the transition probability increases and later the signal level begins to flatten off. The relaxation processes can no longer compete with the increased number of transition as the latter is much faster than the former and hence fewer spins stay long enough in one state to undergo relaxation. Further increase in the microwave power from the steady-state value does not produce appreciable increase in absorption because the steady-state absorption

must be equal to the amount of energy being given to the lattice during relaxation. Eventually the population difference between the levels tends to vanish. The signal increases with power at first, but then the signal-to-noise ratio decreases with increasing power when saturation occurs because the noise produced by the crystal increases with the current passed.[6]

III. 1. THE THEORETICAL HAMILTONIAN

Paramagnetic resonance is concerned with the investigation, in detail, of the lowest energy levels of paramagnetic ions. The energy levels of a paramagnetic ion situated in a crystal are modified by the crystalline surroundings. In order to understand these modifications, one must first have a knowledge of the interactions within the free ion. An attempt is here made to give a brief account of the various interactions. For details reference should be made to Low,[7] Abragam and Pryce[8] and to references (2) and (3).

(a) The most important interaction in an atom is given by the coulomb term which takes into account the interaction of the electrons with the nuclear charge Ze and the mutual repulsion of the electrons. Let this coulomb term be V_F.

(b) The next important interaction is a magnetic interaction between the magnetic moments of the electrons due to its spin and the magnetic moment due to its orbital momentum. Let this be V_{LS}. If we confine ourselves to Russell-Saunders coupling, the spin-orbit interaction can be written as $\lambda \vec{L}.\vec{S}$ where λ is the spin-orbit constant. λ is found to be a positive quantity if the shell is less than half-full and negative if it is more than half-full.

(c) Another much smaller term is that due to spin-spin interaction, which has been considered by Pryce.[9] Let this be V_{ss} . These three are the dominant terms of the free ion.

(d) If the nucleus has also a spin I and a quadrupole moment Q, this causes further splitting. The interaction with the nuclear spin arises from two causes. The first of these is due to the magnetic interaction with the magnetic moment of the nucleus, given by

$$V_N = 2g_N\beta\beta_N\left[\sum_k \left\{\frac{(\vec{l}_k-\vec{s}_k)\cdot\vec{I}}{r_k^3} + \frac{3(\vec{r}_k\cdot\vec{s}_k)(\vec{r}_k\cdot\vec{I})}{r_k^5}\right\} + \frac{8\pi}{3}\delta(r_k)(\vec{s}_k\cdot\vec{I})\right] \quad (1)$$

Where β_N and g_N refer to the nuclear magneton and nuclear gyromagnetic ratio. The term in the curly brackets describes the dipole interaction between the nuclear moment and the magnetic moments of the electron. The other term denotes the anomalous interaction of the S - electrons with the nuclear spin.

(e) The second nuclear interaction term is due to the electrostatic interaction with the electric quadrupole moment of the nucleus. This term, which is second order in I, is given by

$$V_Q = \frac{e^2Q}{2I(2I-1)}\left[\sum_k \frac{I(I+1)}{r_k^3} - \frac{3(\vec{r}_k\cdot\vec{I})^2}{r_k^5}\right] \quad (2)$$

(f) The interaction with the external magnetic field H is given by

$$V_H = \sum_k \beta(\vec{\ell}_k + 2\vec{s}_k)\cdot\vec{H} = \beta\vec{H}\cdot(\vec{L} + 2\vec{S}) \qquad (3)$$

(g) The direct interaction of the nucleus with H is given by

$$V_h = -g_N\beta_N \vec{H}.\vec{I} \qquad (4)$$

The general Hamiltonian of the free ion is given by the sum of all these seven terms. They are conveniently arranged in decreasing order so that perturbation methods may be used for their calculation. They may be written as

$$\mathcal{H} = V_F + V_{LS} + V_{SS} + V_H + V_N + V_Q + V_h \qquad (5)$$

For a paramagnetic ion placed in a diamagnetic substance another term V_c, which is the electrostatic energy in the field of the neighbouring ions, should be included in equation (5). The level separations of V_F are usually of the order of 10^5 cm^{-1}, V_c, for iron-group, is of order 10^4 cm^{-1}, V_{LS} of order 10^2 cm^{-1}, V_{SS} and V_H of order 1 cm^{-1}, V_N of order 10^{-1} to 10^{-3} cm^{-1}, V_Q of order 10^{-3} cm^{-1} and V_h of order 10^{-3} to 10^{-4} cm^{-1}.

Here one is primarily interested in the lowest level and levels removed from it by not more than a few hundred wave numbers, for higher levels are not occupied at the usual experimental temperatures. This means that one need consider only those levels which arise from the lowest level of $V_F + V_C$ by the perturbations of $V_{LS} + V_{SS}$ etc.

2. The Spin Hamiltonian:-

The Hamiltonian given by equation (5) is, in general, very complicated. The method of carrying out perturbation calculations, especially to the iron group, has been worked out by Pryce[10] and others[8].

One could treat the levels between which transitions occur as isolated and forget higher levels, even though they may influence the ground states considerably. In the case of the free ion, a state with total quantum number J splits into $(2J + 1)$ levels in an external magnetic field. With the same analogy, if transitions between $2S' + 1$ levels are observed experimentally, we may define S' as the "fictitious spin" of the system. We can treat the $(2S' + 1)$ levels as if they originate from a fictitious state with spin S' for which the magnetic dipole has $2S' + 1$ possible orientations. The effective moment of this dipole is not given by the Lande' g - factor but by a g-factor which may differ considerably from it. In the case of Cr^{+++} where

the true spin S and the fictitious spin S′ are both equal to 3/2 the g-factor is 1.9800 in a cubic field. But in the case of Co^{++} where true spin S = 3/2 and fictitious spin $S' = \frac{1}{2}$ the g-factor is 4.2785 in a similar environment. If S = S′, g = 2.

An easier method of calculation is to introduce fictitious angular momenta. An angular momentum which does little more than describe the multiplicity of a state is assigned to it. This means that an extra factor must be introduced to take into account of the fact that the magnetic moment is different from what would be expected if the fictitious angular momentum was the real one. This allows the state to be treated almost as a pure state, which is a considerable simplification, but it only works if the other levels are sufficiently far away in energy not to have any appreciable effect. The calculation of the matrix elements of the various perturbation operators is simplified by the use of operator equivalents. Angular momentum operators, which are used in the spin Hamiltonian, are considerably simpler to deal with, since there are standard formulae for finding their matrix elements. The arbitrary coefficients, with which the spin Hamiltonian is built, will express the measured behaviour of the energies of the

transitions when these coefficients are suitably adjusted. The process of determining the coefficients experimentally may be rather long if the number of terms necessary are large, and there is anisotropy.

The advantage of using a spin Hamiltonian is that the rather complicated behaviour of the lowest energy levels of the paramagnetic ion in a magnetic field can be described in a relatively simple way by specifying the fictitious spin, together with a small number of parameters which measure the magnitudes of the various terms in the Hamiltonian.

For a paramagnetic ion placed in the surroundings of a diamagnetic sample giving rise to crystal field of cubic symmetry, the spin Hamiltonian is very simple, being given by

$$\mathcal{H} = g_S \beta \vec{H} \cdot \vec{S} + A \vec{I} \cdot \vec{S} - g_N \beta_N \vec{H} \cdot \vec{I} \qquad (6)$$

Where β_N is nuclear magneton

g_N is nuclear g-factor

A is hyperfine structure constant

and the other quantities are as previously defined.

(3) Spin-Hamiltonian for Co^{++} in MgO:-

Here we discuss the spin-Hamiltonian in brief. For a detailed account of this subject reference should be made to: Abragam & Pryce[8], Low[7] Bowers and Owen[3], Bleaney and Stevens[2] and others listed in the back of the thesis.

The sample which is used for this work consists of Co^{++} ions present in small concentrations in single crystals of Magnesium Oxide, MgO. The Co^{++} ions are surrounded by six oxygen atoms in the crystal, which produce a cubic crystalline field of octahedral symmetry. For this sample each succeeding perturbation is considerably smaller than the previous ones. In most of the cases second order perturbation theory is quite sufficient, but in the case of Co^{++} in MgO the Spin-Hamiltonian is particularly simple.

The size of the crystal field term in the case of Co^{++} in MgO is such that it is small in comparison with the coulomb interaction, but large compared with the Spin-Orbit interaction term, so that the terms may be taken in order. If two terms are of same size the situation becomes complicated since perturbation theory cannot then be used. The method of obtaining the energy level scheme of Co^{++} in MgO is straight forward and follows the standard procedure, so will not be given here. Low[7] has clearly explained how a triplet

is left lowest with 3-fold orbital degeneracy. There is also a small admixture of the upper state into the ground state, which affects the properties of the ground state to some extent. The other neighbouring states are Γ_5 (three-fold degenerate) and Γ_2 with an orbital singlet.

The largest term in the Spin-Hamiltonian is the coulomb term which gives the energy of the coulomb electrostatic interaction of the electrons with the nucleus and with each other. The electron configuration outside closed shells of the divalent Co^{++} ion is $3d^7$ having $^4F_{9/2}$ as the ground state of the free ion. There are three holes in the 3d shell, and $S = 3/2$. The spin multiplicity gives twelve levels as shown in the figure 2. The next highest state is found to be ^4P about 20,000 cm^{-1} higher in energy.

It is found that the ^4P state has the same symmetry properties in the presence of the crystalline field as the ^4F ground state, so that there is a small admixture of ^4P in the ground state, which affects the energy-level spacings slightly.

The next term in the Spin-Hamiltonian is the spin-orbit interaction term. It may be shown that the effect of this term is to remove part of the orbital and spin degeneracy giving a level two-fold degenerate in spin lying lowest.

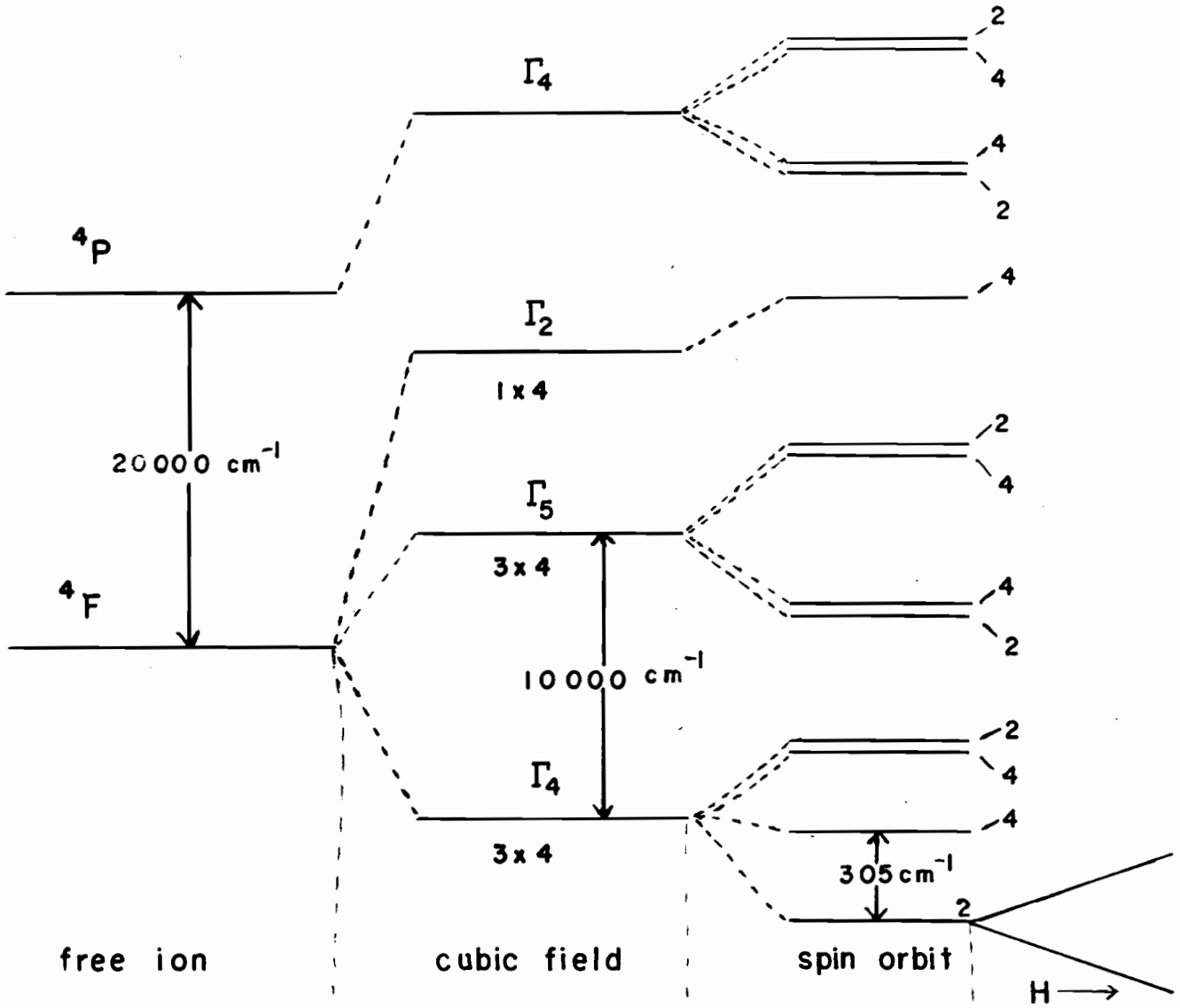

Fig. 2· Energy level splitting of Co^{++} Numbers denote degeneracy.

(Not to scale)

This level with 2- fold degeneracy is split by external magnetic field. Paramagnetic resonance transitions are observed between these two levels at low temperatures at which other levels than the lowest are not populated.

In order to treat this, a fictitious angular momentum ℓ' with total value $\ell' = 1$ and allowed values $m_{\ell}' = 0, +1$ and -1 is introduced. This makes it possible to treat the problem similar to a free atom spin-orbit coupling, except that, since ℓ' is a fictitious angular momentum, the magnetic moment associated with it will differ from that expected from a normal angular momentum by a factor α. If $\vec{J}$ is the resultant of $\vec{\ell}'$ and $\vec{S}$ then the three j values are $j = 1/2, 3/2$ & $5/2$. If these j values are substituted in the equation $\vec{j}^2 = \vec{\ell}'^2 + \vec{s}^2 - 2\,\vec{\ell}'.\,\vec{s}$ in turn, we get $\frac{5}{2}\alpha\lambda$, $\alpha\lambda$ and $-3/2\,\alpha\lambda$ respectively for the spin-orbit coupling term $\alpha\lambda\vec{\ell}'.\vec{s}$. As λ is negative for Co^{++} we see that the term with $j = \frac{1}{2}$ lies lowest. It is between the members of this Kramers doublet that the paramagnetic resonance spectra can be observed. The splitting of the ground state by means of the spin-orbit interaction is also shown in the figure 2.

In second order the spin-orbit coupling mixes in as was already mentioned before, a slight amount of the ^5T triplet state to the ground state. This second order contribution

to the energy is $(\frac{-15}{2\Delta})\lambda$ where Δ is the separation between the two triplet states. This neglects the contribution of the admixture of the P - state, which would amount only to a very slight correction to the already small second order quantity.

The next term in the Spin-Hamiltonian is the spin-spin interaction term. This term, in the present case, has the form $DS_z'^2$ where D is a second-rank tensor. In this case $S_z' = +\frac{1}{-2}$ and the term $DS_z'^2$ is constant with the value 1/4 D. Therefore this may be omitted from the Spin-Hamiltonian since it does not affect the transitions.

The next term we have to consider is the nuclear hyperfine splitting term. Even though the contribution from this term is less than that from the external magnetic field, it is considered first, since it has an effect even in the absence of the field, and is also important in determining the behaviour of the levels as the field is increased. This term arises because of the nuclear spin of the Co^{59} nucleus, which is $\frac{7}{2}$. This has an associated magnetic moment, which possesses energy according to its orientation with respect to the intense magnetic field, of the order of half a million gauss, produced by the ion's unpaired electrons at the nucleus. Hence the energy of the ion depends upon the orientation of the nucleus as well as that of the electrons. For calculation of the interaction

energy between the nuclear angular momentum I and the effective electron spin S' reference may be made to Abragam & Pryce[11], Low[12] and others. The hyperfine structure splitting of Co^{59} in weak and strong magnetic field is shown in the figure 3.

The term responsible for this interaction is of the form $A\ \vec{I} \cdot \vec{S}'$ in the Spin Hamiltonian.

Where $A = \alpha g_s g_N \beta \beta_N \overline{r^{-3}}$ is the hyperfine structure constant. In general A is a second-rank tensor. But in the case of Co^{++} in MgO it may be replaced by a scalar A, since the principal values of the tensor are equal. As shown by the above equation, the hyperfine structure constant, in addition to other quantities, involves $\overline{r^{-3}}$ where r is the distance of the electron from the nucleus. It is possible to obtain an estimate of $\overline{r^{-3}}$ provided g_N is known from other experiments and A is measured experimentally.

(4) The Effect of the External Magnetic Field:-

We are familiar with the behaviour of free spins in an external magnetic field. Ignoring the nuclear hyperfine splitting to start with, let us now consider the effect of external field on the ground state of Co^{++} with the doublet

lying lowest after the effects of the octahedral crystalline field of cubic symmetry and spin-orbit interaction have been taken into account. The effect of the external field is to lift this degeneracy completely. The degeneracy in the upper levels is also lifted though they are not populated at ordinary temperatures at which resonance is possible and hence may be ignored. The two lowest levels diverge linearly with field. At normal fields their separation is not sufficient to bring them appreciably nearer to the higher levels, so that no extra perturbation is introduced.

The above picture is changed due to the presence of nuclear hyperfine interaction. At zero field there are two levels corresponding to $F = 4$ and $F = 3$ separated by $4A$. As the field is increased from zero, these levels split into $(2F + 1)$ equally spaced levels, and hence nine and seven levels respectively are obtained. At high fields F is not a good quantum number and therefore M_s and m_I quantum numbers are assigned to each level. Energy level splitting at high field is shown in figure 3.

The interaction between the quadrupole moment of the cobalt nucleus and the gradient of the electric field at the nucleus is negligible in this case because of zero electric field gradient.

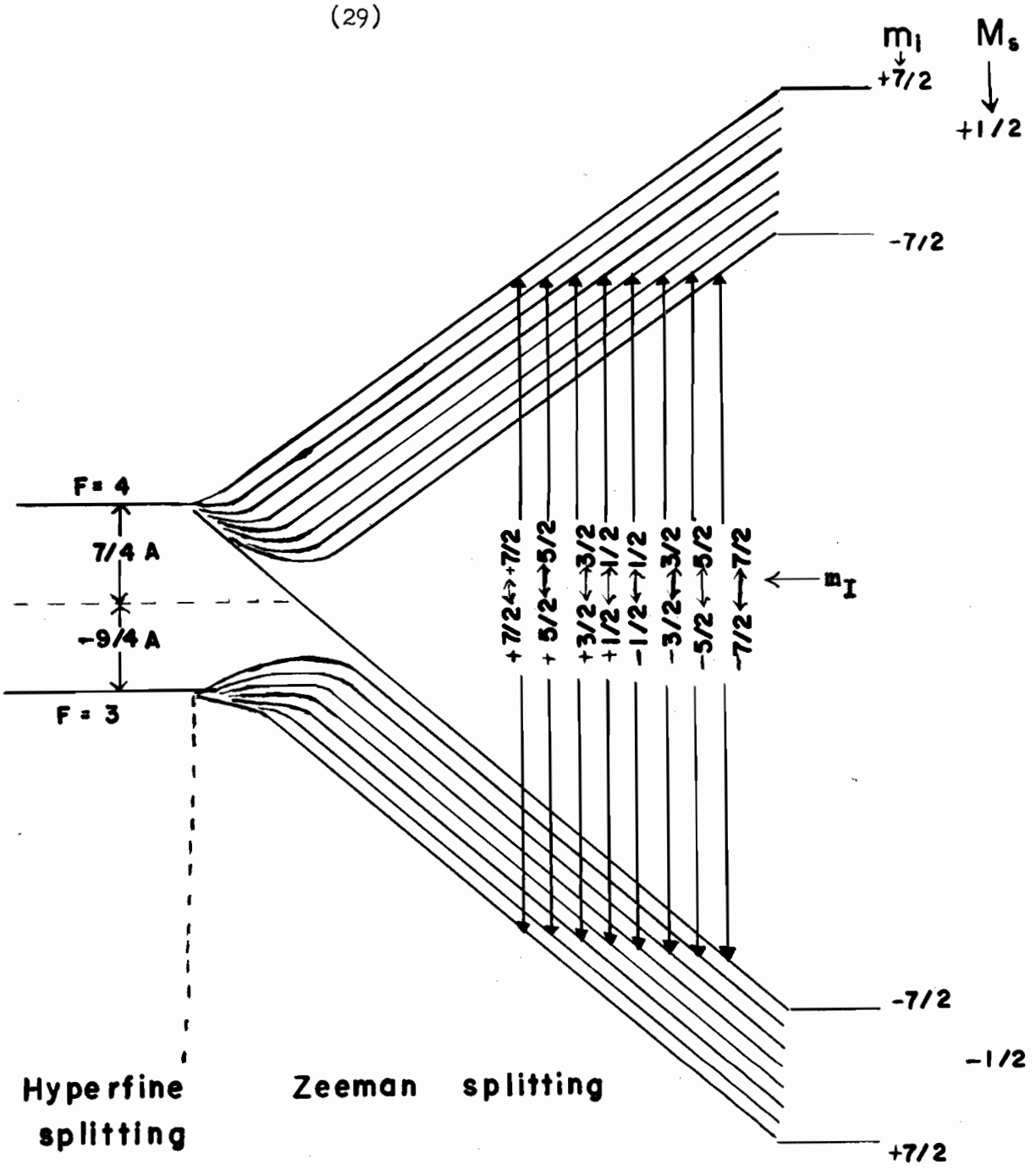

Fig. 3. Effect of External Magnetic Field on Co^{++} in MgO. Arrows Indicate EPR Transitions.

(5) External Field On The Nucleus:-

The effect due to this interaction is quite small. This term is represented as - $g_N \beta_N \vec{H}.\vec{I}$ and is dependent only on the m_I quantum number for a given value of the magnetic field. Thus it does not show up in paramagnetic resonance transitions where, for allowed transitions, the selection rule is $\Delta M_s = \pm 1$ and $\Delta m_I = 0$ as indicated by arrows in figure 3. In addition to the term $- g_N \beta_N \vec{H}. \vec{I}$, we must consider another term of the form $\vec{H}. \vec{I}$ which arises from the next highest state which is separated by spin-orbit interaction. Therefore this term may be written as

$$- g_N' \beta_N \vec{H}. \vec{I} = -g_N \beta_N \vec{H}.\vec{I} - k \vec{H}.\vec{I}$$

$$\text{Where} \quad g_N' = g_N + \frac{k}{\beta_N}$$

Thus knowing g_N, g_N' and β_N the value of k can be found.

The spin-Hamiltonian required to describe the double resonance transition is given by

$$\mathcal{H} = g_s \beta H_z S'_z + A I_z S'_z + A (I_x S'_x + I_y S'_y) - g_N' \beta_N H_z I_z$$

Where the quantization axis and the steady field H are taken to be the Z- direction.

Using this spin Hamiltonian and $S' = \frac{1}{2}$ and $I = 7/2$ the matrix elements are evaluated by using the formula given

by Condon & Shortley[13]. The general matrix elements for the part of the Spin-Hamiltonian, excluding the last term, is given by

$$\langle M_s , m_I | \mathcal{H} | M_s' , m_I' \rangle$$

$$= g_s \beta H_z \langle M_s , m_I | S_z' | M_s , m_I \rangle + A \langle M_s , m_I | I_z \quad S_z' | M_s , m_I \rangle$$

$$+ A \langle M_s , m_I | I_x \; S_x' + I_y \; S_y' | M_s \pm 1 , \; m_I \pm 1 \rangle$$

$$= g_s \beta H_z \; M_s + A \; M_s \; m_I + A \langle M_s | S_x' | M_s \pm 1 \rangle \langle m_I | I_x | m_I \pm 1 \rangle$$

$$+ A \langle M_s | S_y' | M_s \pm 1 \rangle \langle m_I | I_y | m_I \pm 1 \rangle$$

The matrix can be solved exactly to give the energy levels as

$$W \left| \pm\tfrac{1}{2} , k \mp \tfrac{1}{2} \right\rangle = -\frac{A}{4} \pm \frac{1}{2} \sqrt{(k A + g_s \beta H_z)^2 + A^2 \left\{ (I + \tfrac{1}{2})^2 - k^2 \right\}}$$

Where $k = M_s + m_I$; and hence $m_I = k \mp \frac{1}{2}$. k can be considered as a convenient subsidiary quantum number, an extension of the low field quantum number F.

To obtain the correct energy levels for double resonance we still have to consider the term $-g_N' \beta_N \vec{H} . \vec{I}$ which is small, and diagonal, and hence can simply be added to the energy levels already found.

The double resonance energies, with the selection rule $\Delta M_s = 0$ and $\Delta m_I = \pm 1$, are then given by,

$$\Delta W = \pm\frac{1}{2}\sqrt{(kA + g_s\beta H_z)^2 + A^2\left\{(I+\tfrac{1}{2})^2 - k^2\right\}} \pm g'_N \beta_N H_z$$

$$\pm\frac{1}{2}\sqrt{([k+1]A + g_s\beta H_z)^2 + A^2\left\{(1+\tfrac{1}{2})^2 - (k+1)^2\right\}}$$

For calculating the energies, or frequencies, the method devised by Pryce may be used. The double resonance frequency is given by

$$\nu_2 = \frac{A}{2} + x\frac{A^2}{(\nu_1 + g'_N\beta_N H_z)} + y\frac{A^3}{(\nu_1 + g'_N\beta_N H_z)^2} + z\frac{A^4}{(\nu_1 + g'_N\beta_N H_z)^3}$$

$$\pm g'_N\beta_N H_z$$

Where ν_1 is the microwave frequency. Here all quantities are expressed as frequencies rather than as energies. The values of coefficients x, y and z have been given by Pryce (private communication) and reproduced by D.J.I. Fry in his thesis. By using the above formula the double resonance frequencies for Co^{++} in MgO have been calculated in the same thesis. The double resonance transitions obeying the selection rules $\Delta M_S = 0$ and $\Delta m_I = \pm 1$ are indicated in figure 4. by open arrows along with EPR transitions indicated by solid arrows.

The table of x, y and z necessary for ν_2 calculations is not given here because only one line was used in this work, so the positions of the rest are not very important.

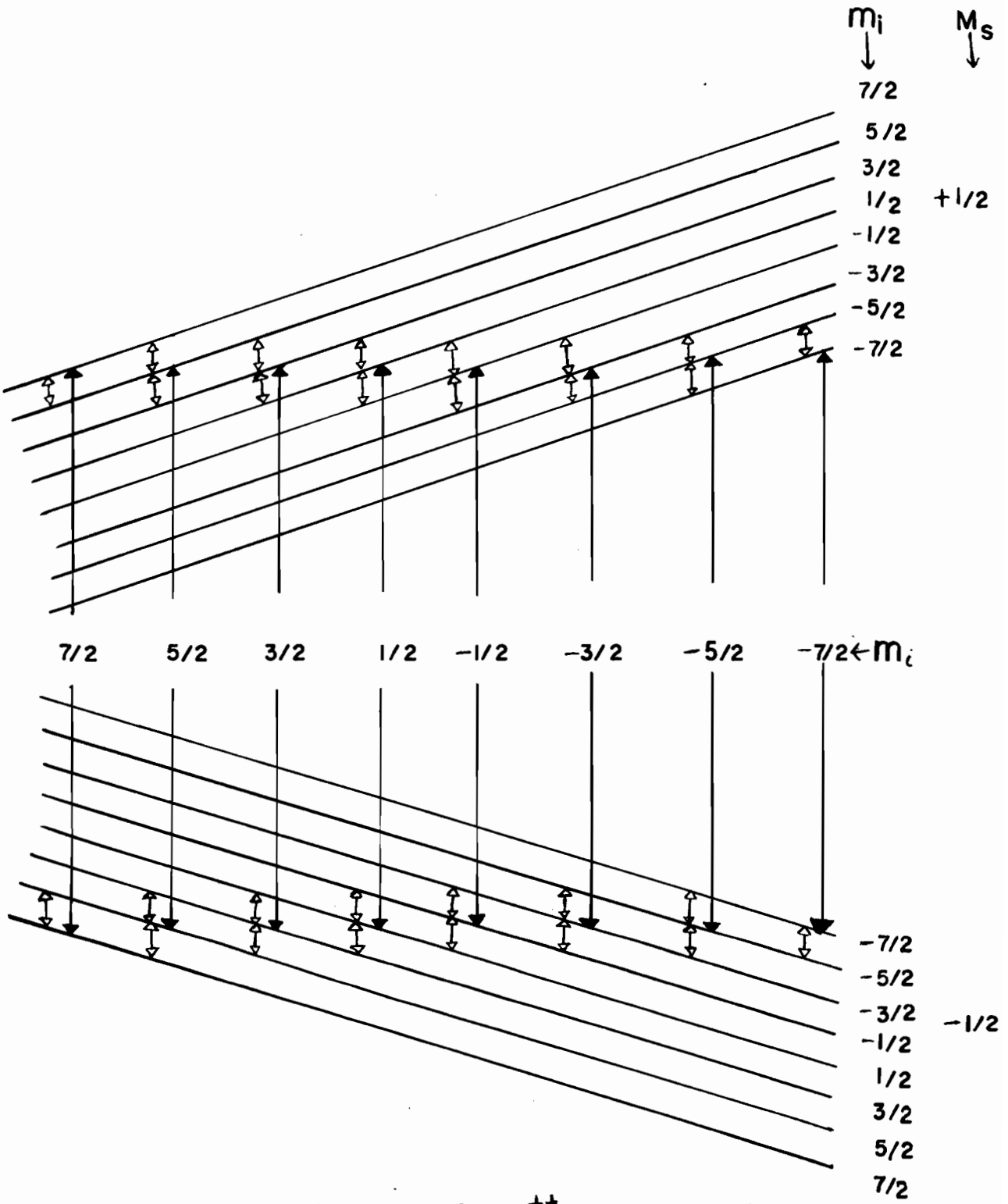

Fig. 4. Energy levels of Co^{++} at high field showing the double resonance transitions.

IV. 1. ENDOR PRINCIPLE

The ENDOR Technique depends upon the presence of the term of the form $A\ \vec{I}\cdot\vec{S}'$ in the Spin-Hamiltonian which is responsible for $(2I + 1)$ equally spaced (if we neglect the quadrupole effects etc) hyperfine levels for every electronic level. This technique, developed by Feher,[14] permits direct measurement of transitions between hyperfine levels in paramagnetic resonance spectra. For double resonance, all that is needed, in addition to a system capable of giving paramagnetic resonance, is a number of fairly close hyperfine levels between which transitions can be induced.

To understand the principle let us consider a simple system with $I = \frac{1}{2}$ and $S = \frac{1}{2}$ for which the hyperfine structure is resolved. The same treatment can be extended to Co^{++} in MgO with $I = 7/2$ and $S' = \frac{1}{2}$. However for understanding the principle the simple system considered above is adequate. In this simple example there will be two levels (in zero field) separated by the hyperfine structure constant A. When a small field is applied, the upper level $(F = 1)$ splits into three equally spaced levels and the lower level $(F = 0)$ is unaffected to start with. As mentioned before the magnetic quantum numbers M_s and m_I are to be used at high field rather than the quantum number F. As the field is increased further the interaction between H and the electronic spin becomes

comparable with and then exceeds the interaction between nuclear spin and electronic spin. The situation is then best described in terms of two levels corresponding to the two possible orientations of the electron spin, with each level subdivided into two, because of the two possible orientation of the nucleus.

Let us now consider the population of these levels. Let us suppose N to be the total number of electron spins. The energy difference between two levels of the same M_s is considered to be negligible in comparison with ΔE, the energy of microwave transition. Therefore, the population of:

both the upper levels $= \frac{N}{4}(1-\epsilon)$ and the population of both the lower levels $= \frac{N}{4}(1+\epsilon)$ at thermal equilibrium

$$\therefore \frac{\text{population of any one of the upper levels}}{\text{population of any one of the lower levels}} = \exp^{-}\left(\frac{\Delta E}{KT}\right)$$

$$\text{i.e. } \left(\frac{1-\epsilon}{1+\epsilon}\right) = \left(1-\frac{\Delta E}{KT}\right) \quad \text{If } \Delta E << K\,T$$

$$\text{or } \quad 2\epsilon = \frac{\Delta E}{KT}$$

Here 2ϵ is the electronic Boltzman factor. This is represented schematically as shown in figure 5(a).

If microwave energy, with quanta of energy $h\nu$, of low power is now applied, electronic transitions satisfying the selection rules $\Delta M_s = \pm 1$ and $\Delta m_I = 0$ are induced and we get two absorption lines at the appropriate field.

Due to the fact that as many spins are going to the upper state by absorption as are going down to the lower state by relaxation processes there will not be any change in the population between levels of the same m_I .

This picture changes if the microwave power is high because saturation effects now have to be brought in. Hence more transitions upwards than downwards occur and as a result the populations are now as shown at 5 (b). As a result of saturation the absorption signal is reduced by an amount depending upon the spin temperature of the system under consideration. Let the population of the levels marked (2) and (3) now be $\frac{N}{4}(1 + \epsilon/2)$ and $N/4(1 - \epsilon/2)$. The condition for this, which is a doubling of the "spin temperature" of (2) and (3) which follows from equation (13)

$$\frac{n_s}{n_o} = \frac{1}{1 + 2PT_1} = \frac{1}{2}$$

Where n_s, n_o, P and T_1 are as defined earlier.

An examination of the diagram 5(b) shows clearly that the levels of the same M_s (different m_I) now differ in population by $\frac{1}{2}\epsilon$ and hence by applying a radio frequency field of correct frequency, transitions of the type $\Delta M_s = 0$ and $\Delta m_I = \pm 1$ between these levels may now be induced. These transitions are "ENDOR" transitions

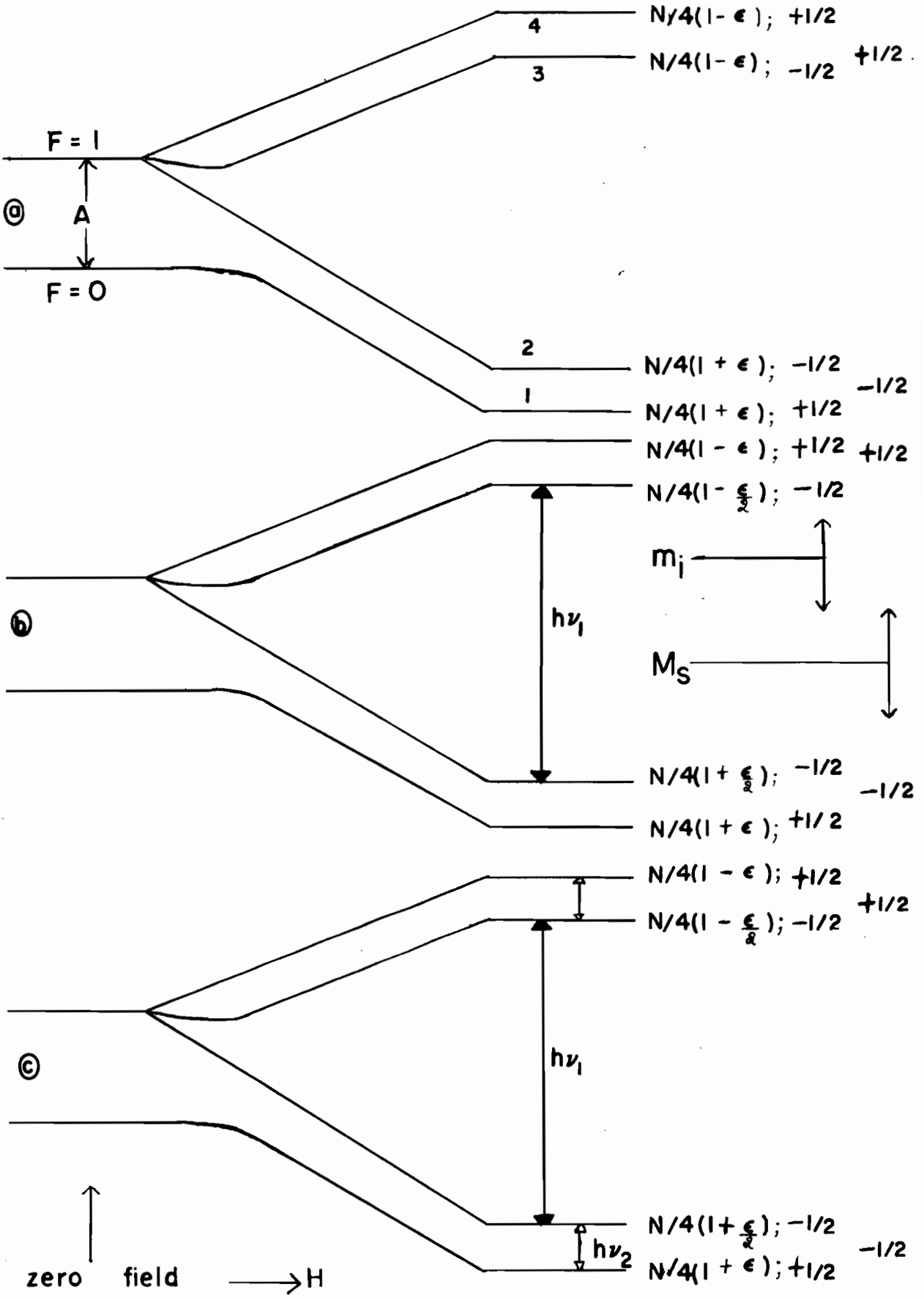

Fig. 5. Explanation of ENDOR technique.

shown as $h\nu_2$ in figure 5 (c) and by open arrows in figure 4 for Co^{++} in MgO. As a result of these transitions between (1) and (2) a few spins go from (1) to (2) and thence to (3) thus enhancing the EPR absorption line. Hence the receiver used for EPR serves as a receiver for ENDOR also because it is the enhancement of EPR signal which indicates the occurrence of ENDOR transitions.

(2) Conditions for a good "ENDOR" Signal:-

The following treatment is that due to P.M.Llewellyn, reproduced by D.J.I. Fry[6] in his thesis:

The signal produced by the crystal rectifier as a result of the change in incident microwave power is considered. It is the change in voltage δV across the rectifier which is important.

Signal $\delta V = \delta I \cdot \bar{R}$

where δI is the change in crystal current, and $\bar{R}$ the average resistance of the rectifier over the range of current δI, $\bar{R}$ being treated as independant of the microwave power p, which is a reasonable approximation if the change in power is very small. Two cases arise.

(a) Linear Region:-

In this case the rectified power is proportional to the incident power, so that,

$$\text{Signal } \delta V = f(p)$$

$$I^2 \propto p; \quad \partial I \quad \delta I \propto \delta p; \quad \delta I \propto \frac{\delta p}{(p)^{\frac{1}{2}}}$$

$$\therefore \text{Signal } \delta V = K\left(\frac{dp}{p}\right)(p)^{\frac{1}{2}}$$

$\frac{dp}{p}$ is the absorption coefficient of the specimen, which is dependent on T_s, the "Spin-temperature", as $\frac{dp}{p} \propto \frac{1}{T_s}$

Hence, Signal $= \frac{A \cdot (p)^{\frac{1}{2}}}{T_s} = \frac{C H_1}{1 + BH_1^2}$

Where A, B, C are constants, $B = \gamma^2 T_1 T_2$ and H_1 is the intensity of the microwave magnetic field.

The condition for maximum signal is $\frac{d\,(\text{signal})}{d H_1} = 0$; which gives $1 - \beta H_1^2 = 0 = 1 - \gamma^2 H_1^2 T_1 T_2$

But $\frac{n_o}{n_s} = 1 + H_1^2 \gamma^2 T_1 T_2$ Refer to Page 13

Where n_o and n_s are as defined on page 9 and 13 respectively. The excess population n which follows the Boltzmann distribution (see page 9) is given by

$$n \cong N \frac{\Delta E}{2 kT}$$

$\therefore \frac{n_s}{n_o} = \frac{T_B}{T_s}$ where T_B is bath temperature, the temperature of the lattice

Thus the maximum signal is obtained when:-

$\frac{T_s}{T_B} = \frac{n_o}{n_s} = 1 + H_1^2 \gamma^2 T_1 T_2 = 2$ which is doubling the spin temperature.

(b) Square-Law Region:-

The rectified voltage is now proportional to the incident power, so $I \propto p$

and signal $= \frac{Ap}{T_s} = \frac{D H_1^2}{1+\beta H_1^2}$ where D is a constant

The condition $\frac{d\ (\text{Signal})}{d\ H_1} = 0$ can only be met by $H_1^2 \to \infty$

so the optimum signal is obtained with the maximum power available.

In general, $\frac{T_s}{T_B} = \frac{1}{1-n}$ for maximum signal where the detecter law is given by $I \propto p^n$.

V. APPARATUS

As EPR is the necessary pre-requisite of "ENDOR", we may say that the "ENDOR" spectrometer is essentially an EPR spectrometer with the necessary equipment and arrangements added to make it possible for the second frequency power to be applied into the cavity in a direction perpendicular to the microwave field at the sample and also to the D.C.magnetic field. As there is already enough literature[15] about paramagnetic resonance spectrometers, it is justifiable here to give only a brief account of the essential parts followed by a description, in detail, of the parts of the spectrometer used to induce double resonance transitions.

(1) EPR Spectrometer:-

The electron paramagnetic resonance spectrometer which is used here is the highly sensitive superheterodyne type. The main parts of such a spectrometer are

(1) A monochromatic source of microwave power tunable through a range of 7,500 to 10,3000 Mc/s.

(2) A resonant cavity in which the sample to be studied is put.

(3) Variable D.C.magnetic field.

(4) Receiver with display system.

(5) Equipment necessary for work at low temperatures.

(6) A precision wave-meter, a power meter and a frequency counter etc - i.e.; calibrating and measuring equipment.

A block diagram of a spectrometer employing superheterodyne detection system is shown in figure 6 along with the parts required for a double resonance spectrometer.

The source for supplying microwave power is a sperry 2k39 klystron. It is necessary that the frequency of the klyston must be kept constant. This is achieved by the pound stabilizing unit by which it is possible to obtain a short-term stability of one in 10^8. Actually our stability is 1 in 10^6. For operational details of this unit and for a block diagram reference should be made to R.V. pound[16] or any standard book on microwave spectroscopy. The operating frequency is fixed at about 9200 Mc/s and the power output from this klystron is about 200mw. The power incident on the cavity can be measured with an H.P. 430 CR power meter after being connected to it through a 20 db directional coupler as shown in the block diagram. The power incident on the cavity can be controlled by means of a calibrated attenuator.

(2) Cavity: The resonant cavity is the place where absorption of microwave power by the sample takes place resulting in the change of Q of the cavity, It was intended to use a transmission cavity, but a reflection cavity was used for these experiments. The original transmission cavity, which allowed exclusion of liquid helium had a rather low Q, and the receiver developed faults, which made it desirable to use instead the reflection system which had been built up.

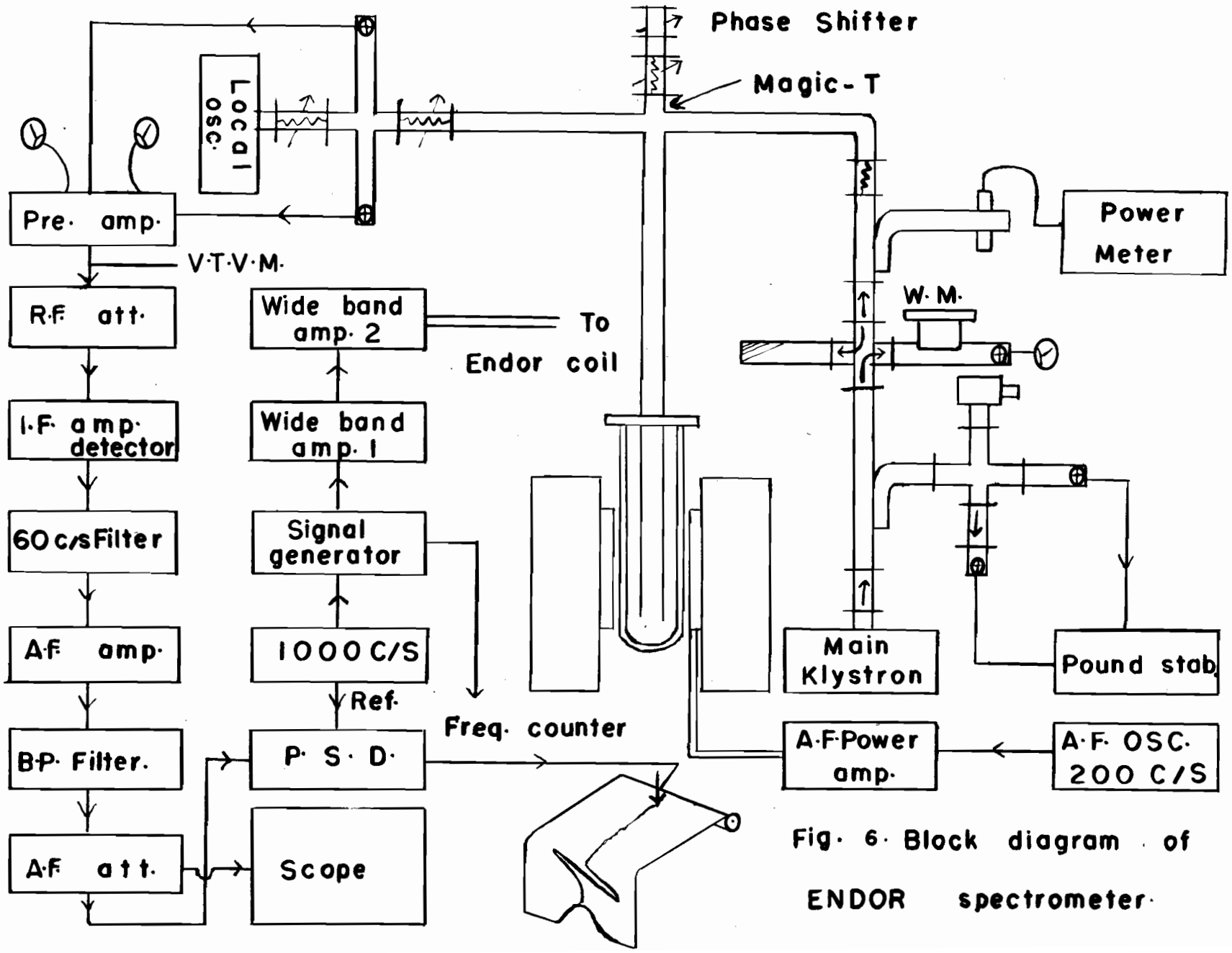

Fig. 6. Block diagram of ENDOR spectrometer.

ENDOR was first obtained with the transmission system, but after rather mysterious faults developed, the reflection system was much better, and so used in preference. A reflection cavity, based on that used by R.W.Terhune[17] et al, was designed by Mr. A. Manoogian. This was cut out of a copper waveguide piece $(\frac{1}{100})''$ thick, coupled to the rest of the waveguide through a coupling hole of approximately $(\frac{5}{16})''$ in diameter. By a moveable plunger, with the inner surface polished, this could be tuned over a certain range of frequencies. The mode used is the rectangular TE_{102} mode, one wave length long. The cavity has a fairly high Q and can be used alternatively either as an EPR cavity with high frequency modulation of the steady magnetic field with a slight modification or as a double resonance cavity.

(3) ENDOR Coil:-

It is through this coil that one can feed the second frequency power for inducing double resonance transitions. The coil is made of very fine copper wire and has two turns of radius 1/3 cms wound round a flexible teflon film formed in the shape of an almost circular tube. One end of this two-turn coil is connected to a piece of phosphor-Bronze wire of diameter $\lesssim$ 0.020" which is the central conductor of

the coaxial cable. The outer conductor of the coaxial cable is 3/16" in diameter, thin-wall cupronickel tubing. Insulation is provided by polyethylene from a normal coaxial cable, the centre hole being large enough for the phosphor-Bronze wire to be pushed through. By using just a single piece of polyethylene, fair support is provided at all points for the centre conductor, reducing the likelihood of troublesome microphonics. Termination at the upper end is made by a standard coaxial plug to which, output from the second wide-band amplifier is connected. The second frequency coil is introduced into the cavity through a circular hole of diameter about $\frac{(5)}{16}$" cut in the centre of the broad-side of the cavity as shown in the figure 7. - The microwave field configuration is shown in figure 8 (a), and figure 8 (b) shows the directions of the microwave field H_1, second frequency field H_2 and the D.C.magnetic field H at the sample, which is fixed in position at the centre of coil.

The main advantage of this cavity over the transmission cavity is that all the three fields are acting at right angles to one another which is complicated to achieve with the transmission cavity. However, the main disadvantages with the reflection cavity used for this work were that there was no provision for pumping on liquid helium and spurious noise due to the boiling helium could not be avoided.

(4) D.C.Magnetic Field:-

The steady D. C. magnetic field is supplied by a varian magnet which has pole-pieces six inches in diameter, and air gap of about 4". A continuous flow of cold water is maintained in the cooling coils which avoids heating up of the coils. The magnet is designed to operate at low voltage and high currents. The whole magnet can be rotated about a vertical axis making it possible to apply the field at any desired angle in the horizontal plane. Field of the order of 6000 gauss can be obtained with this magnet power supply.

In order to get a steady field without any drifts, it is necessary to use magnet current stabilizing system. The stabilization system which is used here holds the field constant to about 1 part in 10^4.

Small coils, of about a hundred turns each, are fitted round the pole-pieces of the magnet. These are the modulation coils used to modulate the steady field as this is necessary during the course of the experiment. With these coils, modulation of up to about two gauss peak-to-peak at 200 c/s can be obtained.

As the frequency is usually maintained constant during the experiment it becomes necessary to vary the D. C. magnetic

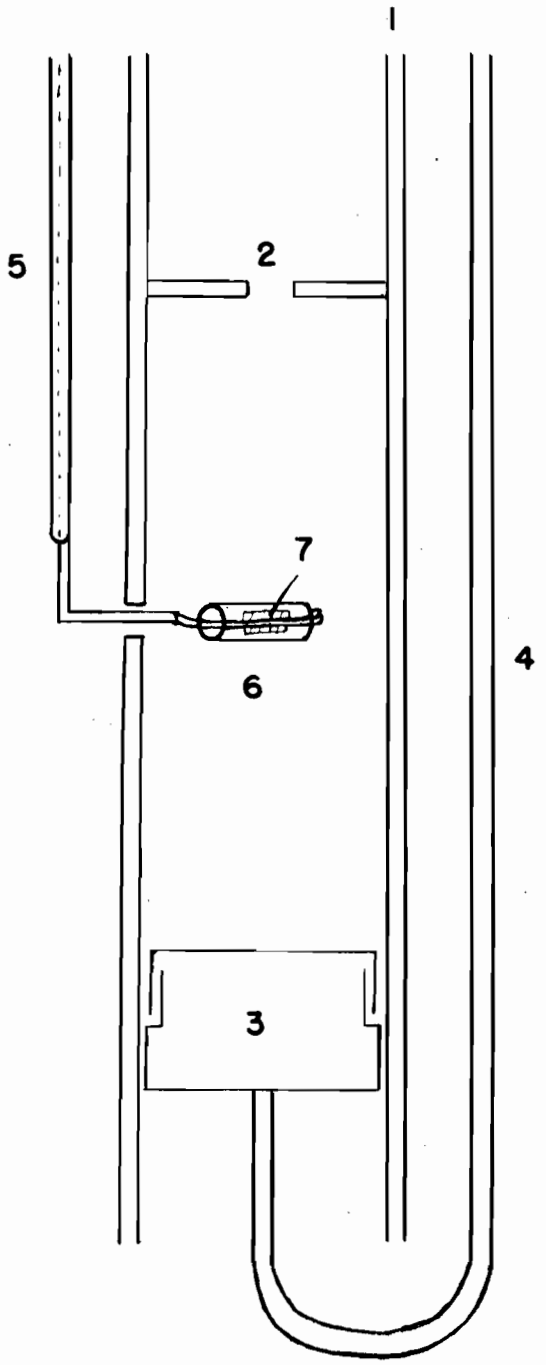

Fig. 7. Endor Cavity

1.= Rectangular Copper wave guide. 2.= Coupling Hole.
3.= Tunable Plunger. 4.= Rod for Tuning.
5.= Cupro-nickel coaxial tube for R.F. Power.
6.= Two-turn Coil for R.F. field.
7.= Sample inside R.F. Coil

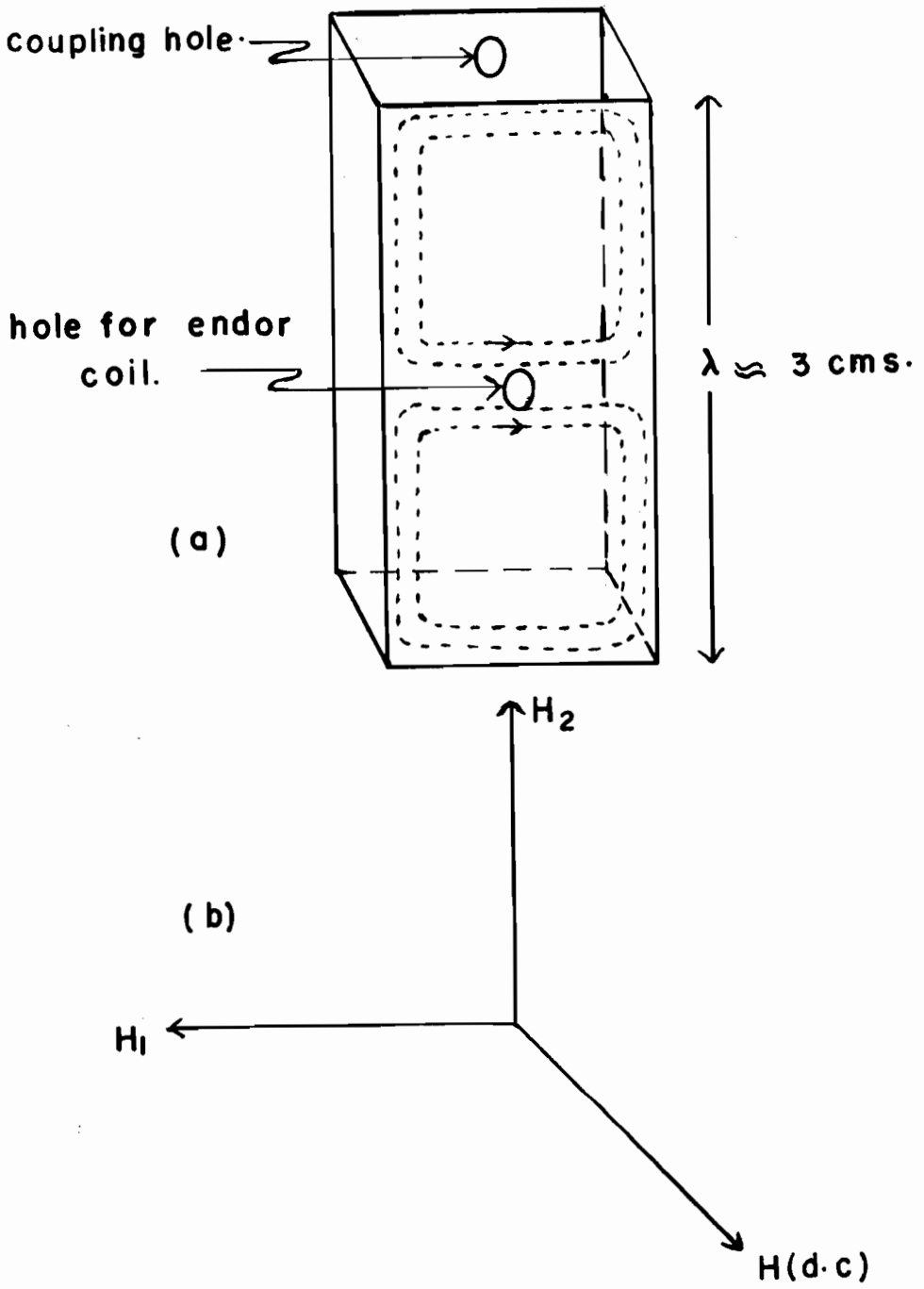

Fig. 8 (a) Showing the microwave field in the cavity
8 (b) Shows the directions of the three fields at the sample.
H_1 is in the horizontal plane, H_2 is in the vertical plane and H is perpendicular to the plane of the paper

field slowly in order to pass through resonance. This is provided for by means of a slowly-varying artificial error signal from the potentiometer, derived from the fine control. The control is a "helipot" which is driven by a clock motor. By this device the D.C. field can be swept with different speeds.

(5) Receiver:-

The function of any receiver is to detect the signal, amplify it to the appropriate level and to make a presentation with reasonable signal to noise ratio. Depending upon the quality of the final signal required there are several methods of detection. The simplest of them is the simple straight detection sensitive to χ''. Under those conditions the crystal current will be proportional to the power transmitted from the cavity. This output from the crystal is then amplified by a high gain audio amplifier and displayed on the scope or chart-recorder which gives the absorption signal. In order to get the signal sensitive to phase the output from the A.F. amplifier is fed into a phase-sensitive detector through the "signal" input and a reference signal from an A.F. oscillator is fed into P.S.D. through "Reference" input. The great advantage of

using a P.S.D. is to the reduction in the band-width and the improvement in signal/noise ratio. This method of detection is simplest and easy to set up, but it is found that it is not sensitive enough for very weak signals.

Superheterodyne Scheme:-

A superheterodyne system is used so that the crystal contributes noise in a narrow band at ~ 30 Mc/s instead of zero frequency. This is advantageous because of the 1/f crystal noise dependence. This method of detection is most sensitive of all the methods and mostly used where accuracy and sensitivity are of primary importance. The method is similar in principle to the superhet radio receiver. An important aspect of the detection scheme is that the conversion loss of the crystal can be reduced by a balanced mixer which balances out local oscillator noise. At frequencies of a few megacycles, the x-tal noise output is very small even at high powers where the conversion gain is large. Using good matched crystals it is possible to minimize local oscillator noise by means of this balanced detection. A superheterodyne scheme usually operates at an intermediate frequency of 30 Mc/sec. This intermediate frequency is obtained by beating the main signal frequency with a local oscillator which differs from the signal frequency

by the intermediate frequency. The limiting factors in the sensitivity seems to be the noise factor of the I.F. amplifier which can be minimized by a very careful design, and the crystal noise.

The superheterodyne detection system used here closely resembles the system used by Feher[15]. The block-diagram of a spectrometer using this scheme has already been shown. The one which was assembled here operates at about 3 cms. wave length (the frequency of operation is round about 9200 mc/s) with a reflection cavity. The signal generator feeds into the magic - T, where its power is distributed between two arms. The lower arm is connected to the cavity with the sample, the reflected voltage being bucked out with the aid of the upper arm of the magic-T. For this purpose the upper arm has a phase shifter and an attenuator, an arrangement which was found to be more satisfactory than a slide screw tuner as far as stability and ease of operation are concerned. The desired signal appears in the arm connected to the balanced mixer. It is now fed into a balanced mixer which receives the local oscillator power from the klyston. The output of the mixer is fed first to a low noise I. F. pre-amplifier and then to an I. F.main amplifier both operating at about 30 Mc/S

with a band width of a few megacycles. There is a detector built into the last stage of the I.F. amplifier after which it leads to a tektronix battery amplifier through a 60 c/s filter which reduces the hum. The output of this battery amplifier, having a gain of about 100, is passed through a band-pass filter and then to one of the terminals of a phase-sensitive detector. The final signal can be obtained on the chart recorder, on which the derivative of the absorption line is traced.

There are provisions for measuring the main klystron power, meters for crystal currents, a V.T.V.M, included through a T-connector after the pre-amplifier for balancing the bridge, and wave meters for measuring frequencies.

(6) Second Frequency (ν_2) Generator and Accessories:-

The equipment outlined above is just the necessary things for observing the electron spin resonance. For observing double resonance, we must have some additional equipment. The main additional part apart from the special type of cavity already described is a signal generator in the required range along with amplifier units of necessary type to provide reasonably high power.

A radiometer, A.M. - F.M. signal generator, type MS27b, with a range of operation from ~1 to 240 Mc-was used in this work. It can be operated at any one of the 0.3 - 15, 15-30, 30-60, 60-120 and 120-240 Mc-ranges. The output level is variable from .1 μV to 100 mv and the output can be drawn through internal impedances of either 50 or 75 ohms. Either amplitude or frequency modulation is available at one kilocycle from an internal source, and the modulation level is variable over a wide range. This is very useful as it is intended to compare the results obtained by A.M. and F.M. There is also provision for using external modulation, either frequency or amplitude. The internal modulation is also used as the reference signal for the phase-sensitive detector when sweeping the second frequency. As the field at the centre of the ENDOR coil is required to be about 1/10 gauss, the output from the signal generator needs amplification before it is fed to the coil. Two wide-band amplifiers are used, connected in series. The band-width of both these amplifiers is between ~5 to 240 Mc. The first amplifier is a CECO, model 1006; and the second amplifier is a I.F.I, model 510. The two amplifiers have a total gain of about 35 db. The maximum output of the two amplifiers in series is about 7 volts r.m.s. $\simeq$ 18 volts, peak-to-peak across a load of 185 ohms. The current $\simeq$ 18/185 amperes and the field at the centre of the coil is given by

$$H = \frac{2\pi x\ n}{10r}\ i$$

Where i = current in amperes

r = radius of the coil

n = number of turns in the coil

And H = is the field in gauss

For the coil used here, we have,

$$r = \frac{1}{3} \text{ cms}, \quad n = 2 \text{ turns}$$

$$\therefore \quad H = \frac{2x\ \pi\ x\ 2}{10\ x\ \frac{1}{3}} \times \frac{18}{185} \text{ gauss} \cong \frac{1}{10} \text{ gauss}$$

Which is of the same order as required. During the course of experiment it is found that the signal is maximum when the output from the wide-band amplifiers is maximum.

EXPERIMENTS AND RESULTS

Many experiments were performed with the intention of understanding, in detail, the behaviour of the spectrometer for ENDOR under different conditions. Samples of MgO containing a small percentage of Co^{++} ions were used. Three different concentrations were investigated. For each concentration, measurements were restricted to the following:

(1) To find out the spin temperature at which a good ENDOR signal could be obtained - i.e. a saturation run, where the saturation of the EPR line and therefore the spin temperature of the levels involved was varied, and the effect on the ENDOR signal noted.

(2) Variation of the ENDOR signal with F.M. deviation.

(3) Variation of the ENDOR signal with percentage amplitude modulation.

(4) Dependence of the ENDOR signal with second frequency (ν_2) voltage, and

(5) To investigate the dependence of ENDOR signal on the saturation level.

The variation of ENDOR signal with F.M., A.M. and ν_2 voltage is expected to be linear for all concentrations.

The variation of ENDOR signal with saturation level, and the optimum value of saturation are expected to be dependent on concentration, and so to differ somewhat from sample to sample.

In addition to the measurements mentioned above, experiments were attempted to find the dependence of the intensity of double resonance signal on the direction of the steady magnetic field with respect to the microwave magnetic field. This was not very successful because the value of D.C. magnetic field at the sample is likely to change slightly on rotating the magnet, requiring tedious re-setting on the EPR line after each change of magnet angle. Such a re-setting then requires re-balancing of the bridge, making the set of measurements very tedious and time-consuming. Measurements were discontinued when it was found virtually impossible to get consistent results. The results would be of interest, and it is intended that the measurements will be made when improvements in the equipment have been made, and the reliability of the measurements increased. Also, attempts to measure the double resonance line-width and its dependence on concentration were not very encouraging because of some difficulties encountered in accurate measuring of the ENDOR frequencies. The trouble with line-width measurement is due largely to the shape of the line - the maximum and minimum points of the differential line-shape are not very well defined. The centre of the line, however, where the trace intersects the zero, is very clear and allows much greater accuracy of measurement, as indicated by the figure 9 .

(1) Saturation Run:-

To find the optimum settings for a good double resonance

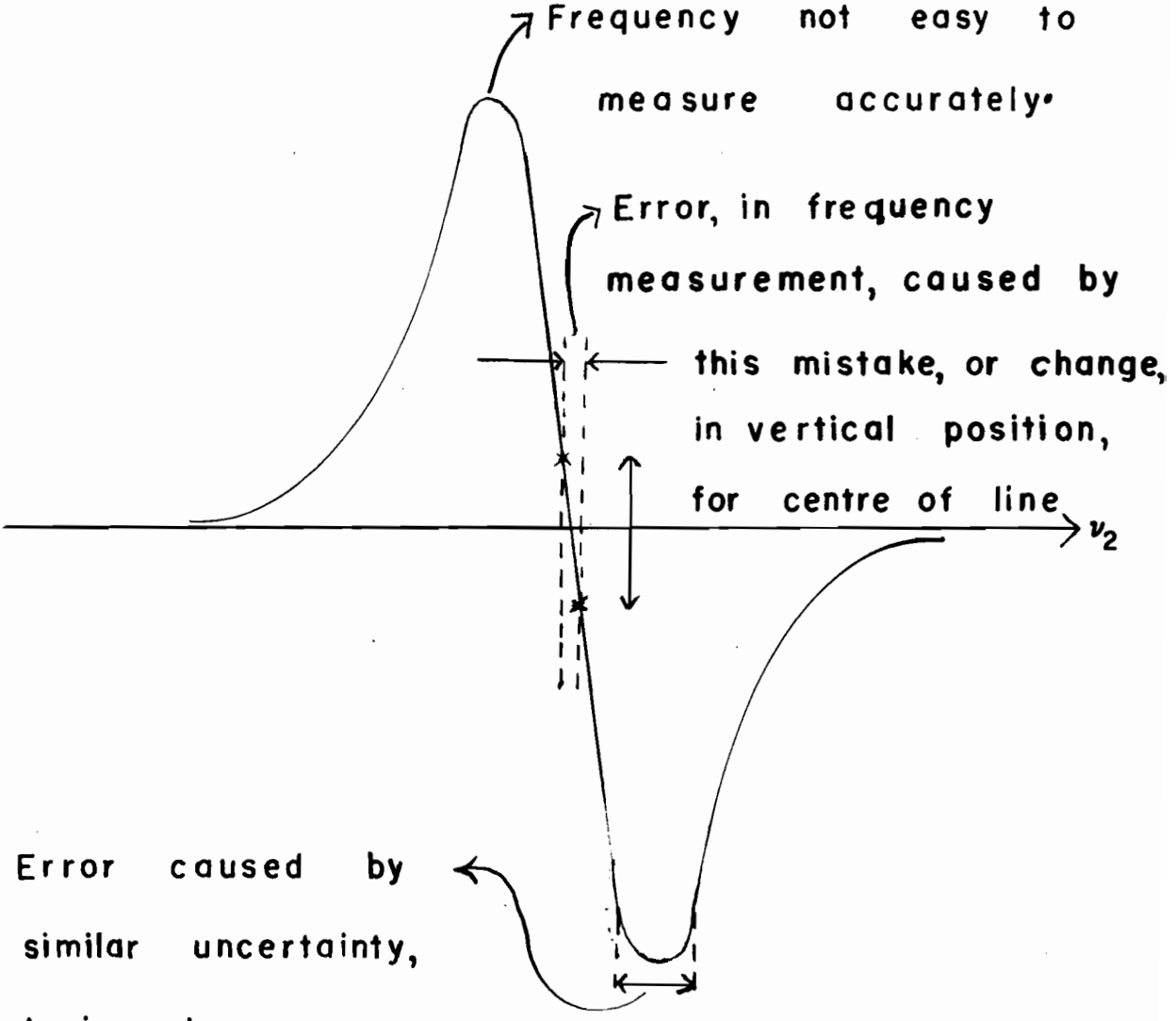

Fig. 9. Indicating difficulty of line-width measurement.

signal the usual saturation technique is followed. It is expected that a reasonably good double resonance signal results when the spin temperature is doubled. To find out the settings which correspond to this doubling of the spin temperature the following procedure is followed.

With the three fields, i.e. steady field H, the microwave (γ_1) field H_1 and the second frequency (γ_2) field H_2 at right angles to one another, and when the sample is at liquid helium temperature the cavity is tuned for cavity resonance. The local oscillator frequency is adjusted until the vacuum tube voltmeter reads a maximum. The microwave bridge in the dummy arm of the magic -T has now to be balanced. To achieve this, the attenuator and the phase control of the microwave bridge are adjusted in turn until a minimum reading on the vacuum tube voltmeter at the output of the pre-amplifier is observed. With this adjustment, the output of the magic -T should be almost proportional to χ'' . It is now necessary to have a good combination of the settings of the various attenuators which are positioned in the system as shown by the block diagram of figure 10. The sum of the microwave "pre"-attenuator and the microwave "post"-attenuator settings is always kept constant in order to keep the power level at the input of the superheterodyne receiver as near constant as possible. In the course of a saturation run it is also necessary to keep the I.F. attenuator constant.

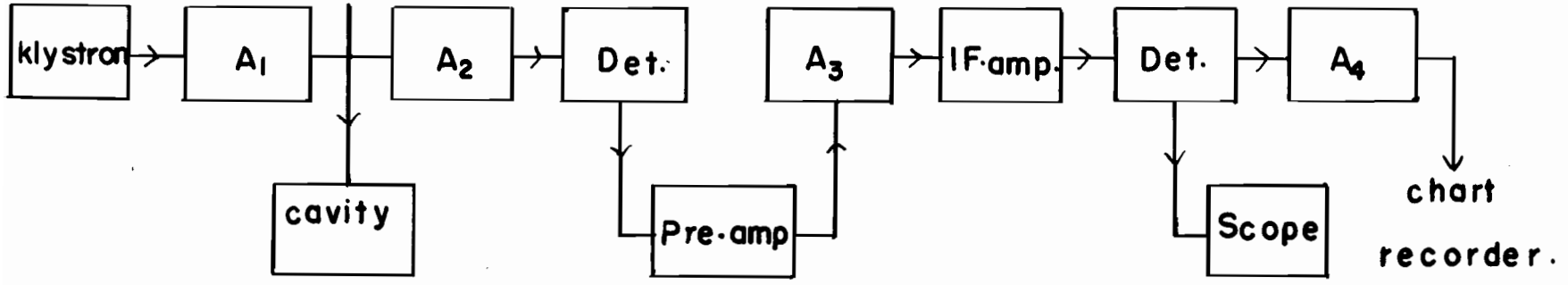

Fig.10. Block diagram showing positions of the various attenuators in the system.

The attenuators A_1 and A_2 are set with a total attenuation of 40 to 60 db, this amount being necessary to ensure that the I.F. amplifier is not saturated when the normal amount of attenuation (60 db) follows the I.F. pre-amplifier. A good trace on the chart recorder is usually obtained with 50 db attenuation before the signal cavity.

Traces of the signal are now taken as the attenuation before the cavity is reduced in steps, i.e. the power incident on the cavity is increased. The total attenuation in the microwave line is kept constant (apart of course from changes in the cavity itself) by adjusting the microwave "pre"- and "post" attenuators together so that the sum of their contributions to the attenuation is constant. At least two sets of readings are taken for each point on the graph and their mean calculated. A graph, for each sample, with the intensity of the signal plotted against the power incident is shown on graph 1. From the graphs approximate settings of the microwave "pre"-attenuator for getting a good ENDOR signal can be found. The table on page 62 gives the settings of the various attenuators for EPR and ENDOR signals.

Referring to the graph for the 5% nominal Co^{++} in MgO sample shows that the intensity of the signal remains fairly constant until the incident power is about 30 db below 1 watt. Any further increase in the incident power saturates the EPR

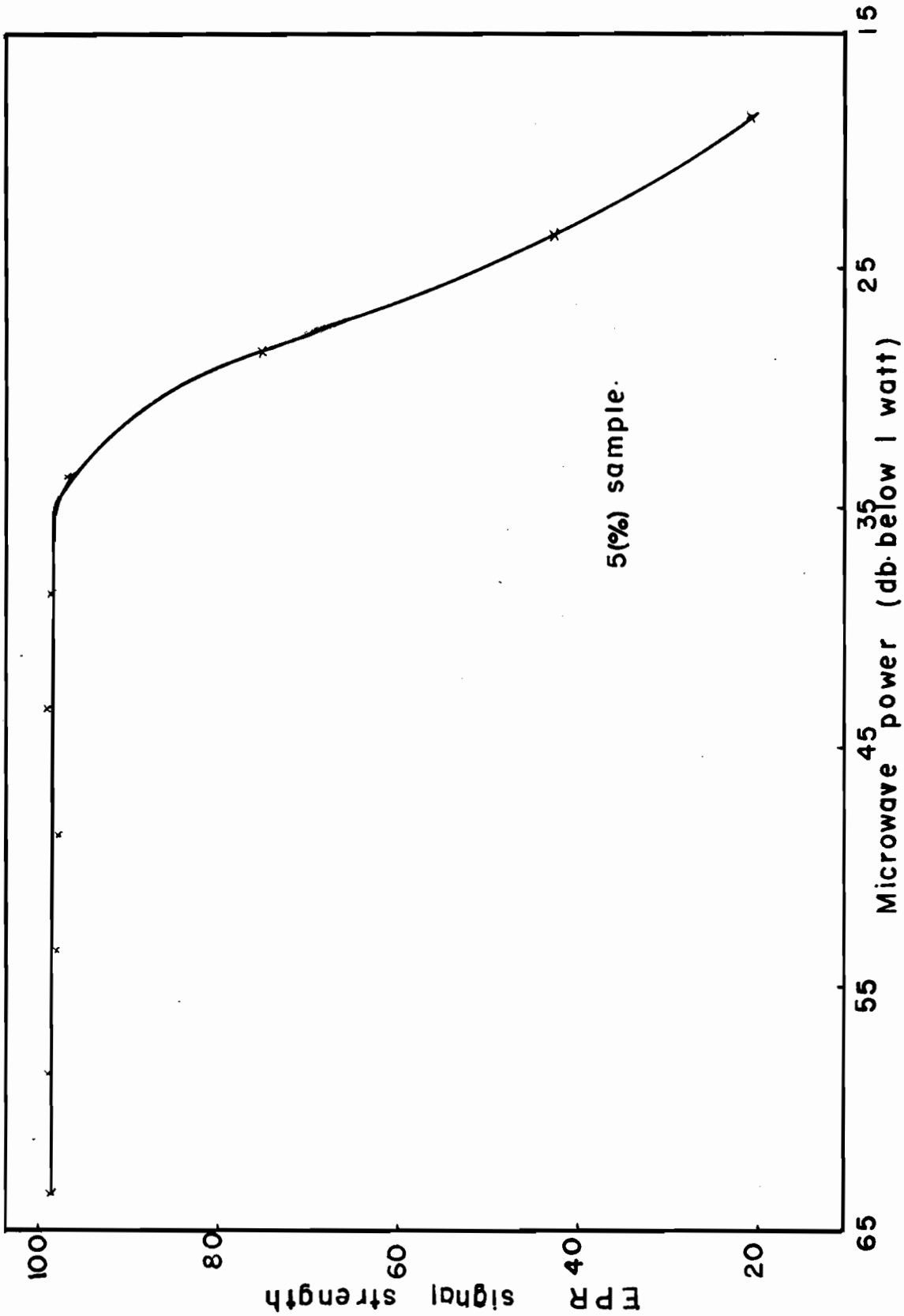
EPR signal strength
100
80
60
40
20
65
55
45
35
25
15
Microwave power (db. below 1 watt)
5(%) sample.

Graph 1.

Concentration %	Frequency Mc ν_1	EPR Settings in db. A_1	A_2	A_3	A_4	ENDOR Settings in db. A_1	A_2	A_3	A_4
5%	9186	50	10	60	25	10	20	60	25
2%	9190	50	0	62	20	12.5	12.5	62	32
.5%	9186	40	0	60	20	17.5	7.5	50	15

TABLE:- Settings of the various attenuators for EPR and best double resonance signal.

A_1 - pre-attenuation; A_2 - post-attenuation.

A_3 - I.F. attenuation; A_4 - A.F. attenuation.

signal as shown by its decreasing magnitude. Doubling the spin temperature corresponds to about 24 db below 1 watt which agrees quite well with that of the ENDOR settings used while performing the experiments as shown in the table.

The saturation curve of the 2% nominal sample in graph 2 indicates that the EPR signal remains fairly constant before it gradually falls. The signal falls by more than 50% when the incident power exceeds 26 db below 1 watt which also agrees with the value given in the table. The table corresponds to the settings at which most of the measurements were made.

For the low concentrated sample the saturation curve is as shown in the graph 3.

Some of the points are slightly away from the curve drawn. This may be due to noise inherent in the electronics. Apart from this, the curves seem to be reasonably good and reproducible.

The transition studied for all the above experiments is $m_I = -7/2 \longleftrightarrow -7/2$

and $M_s = \frac{1}{2} \longleftrightarrow -\frac{1}{2}$

(2) <u>General Remarks on ENDOR Measurements</u>:-

For all the measurements undertaken in the course of this work the transition $m_I = -\frac{5}{2} \longleftrightarrow -\frac{7}{2}$ corresponding to $M_s = -\frac{1}{2} \longleftrightarrow -\frac{1}{2}$ was studied. Out of the two expected ENDOR lines at frequencies

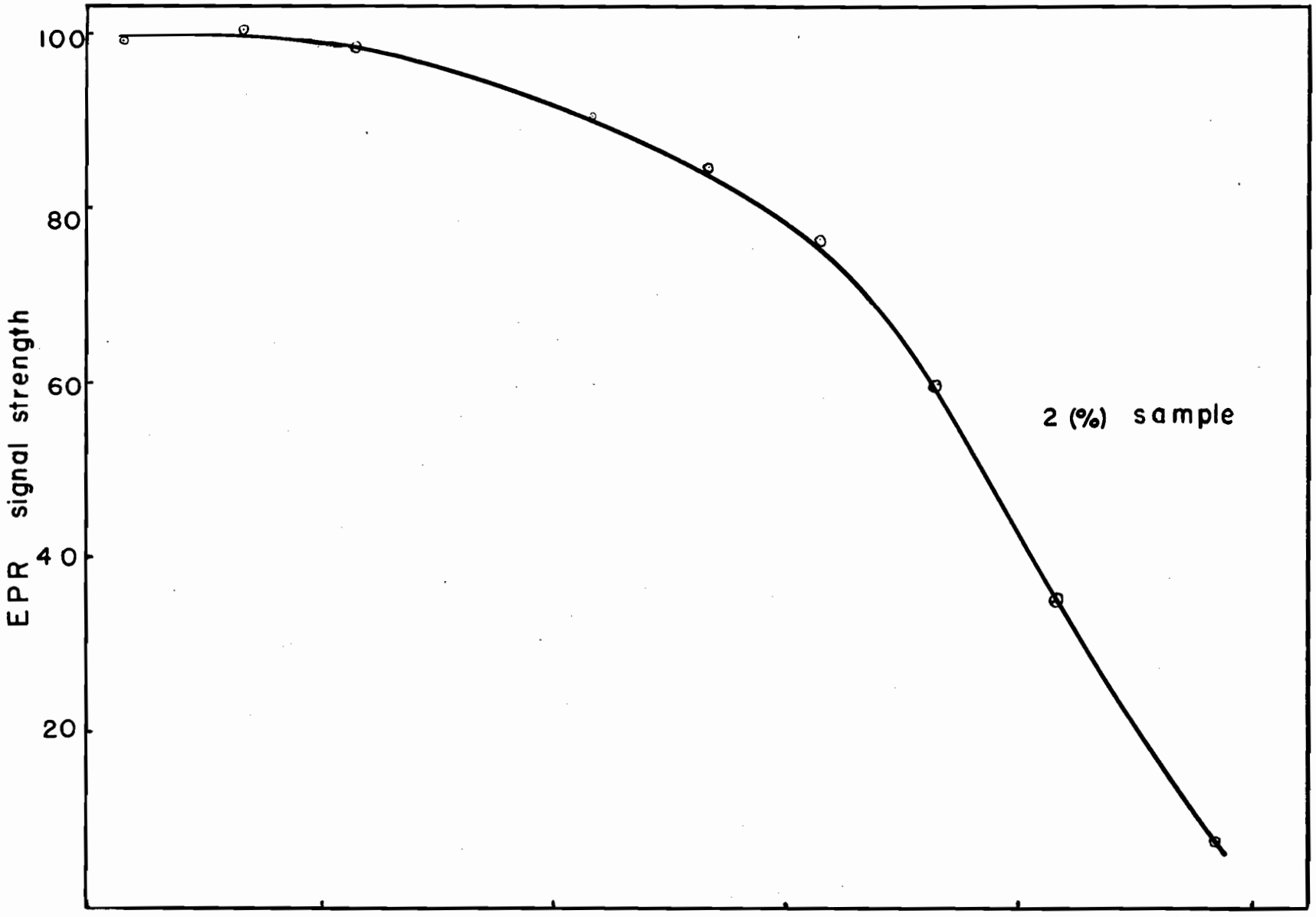
100
80
60
40
20
EPR signal strength
2 (%) sample
65
55
45
35
25
15
Microwave power (db. below 1 watt)

Graph 2.

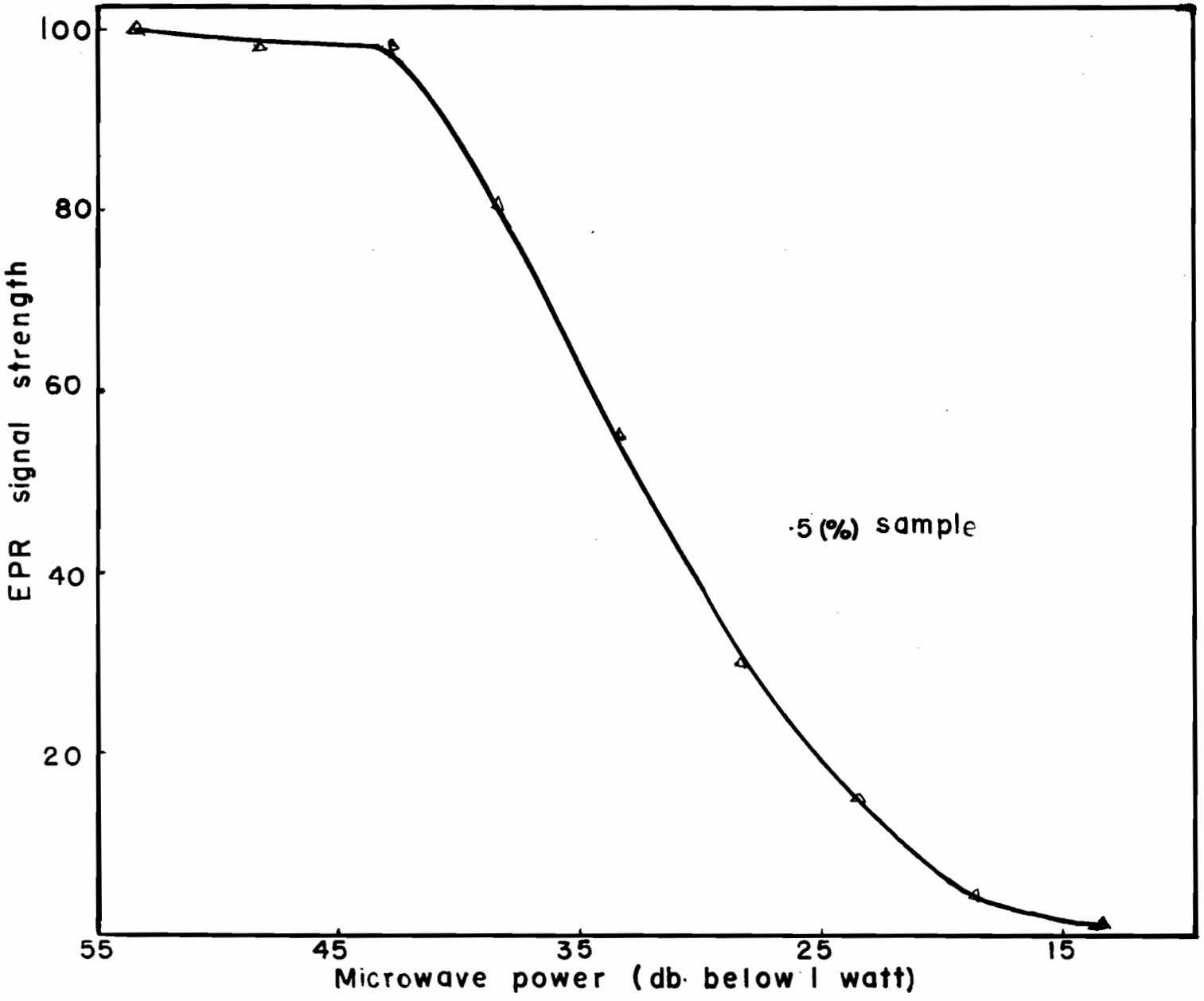
100
80
60
40
20
EPR signal strength
·5 (%) sample
55
45
35
25
15
Microwave power (db below 1 watt)

Graph 3.

152.89 Mc/s and 163.00 Mc/s, measurements were made on the one appearing at 163 Mc/s. It was found that more double resonance lines than those predicted above by the simple theory were observed. Some of the ENDOR lines observed, along with the approximate frequencies at which they occur, are shown in the figure 11 . It was also found that more concentrated the sample was, the more were the "unexpected" ENDOR lines observed which is in confirmation of the work done by D.J.I. Fry and P.M. Llewellyn at Bristol.

(3) Dependence of Double Resonance Signal With F.M.Deviation:-

The effect of frequency modulation on the double resonance signal is analogous to the modulation of the steady magnetic field when observing a paramagnetic resonance signal. If the modulating field is small compared with the line-width of the EPR signal it is found that the signal strength varies linearly with the amount of modulation. If the modulating field is comparable with the width of the EPR signal then the signal will be distorted and hence deviation from linearity occurs. And in the ENDOR case, F.M. behaves just like field-modulation for EPR i.e. if F.M. deviation is too large, it distorts and broadens the ENDOR line. The ENDOR signal should be linear up to 100% A.M. (provided the signal generator does not give distortion).

The signal generator used had internal modulation at 1000 c/s, F.M. or A.M. of adjustable amount, with a meter monitoring percentage A,M. or F.M. deviation. It was thus

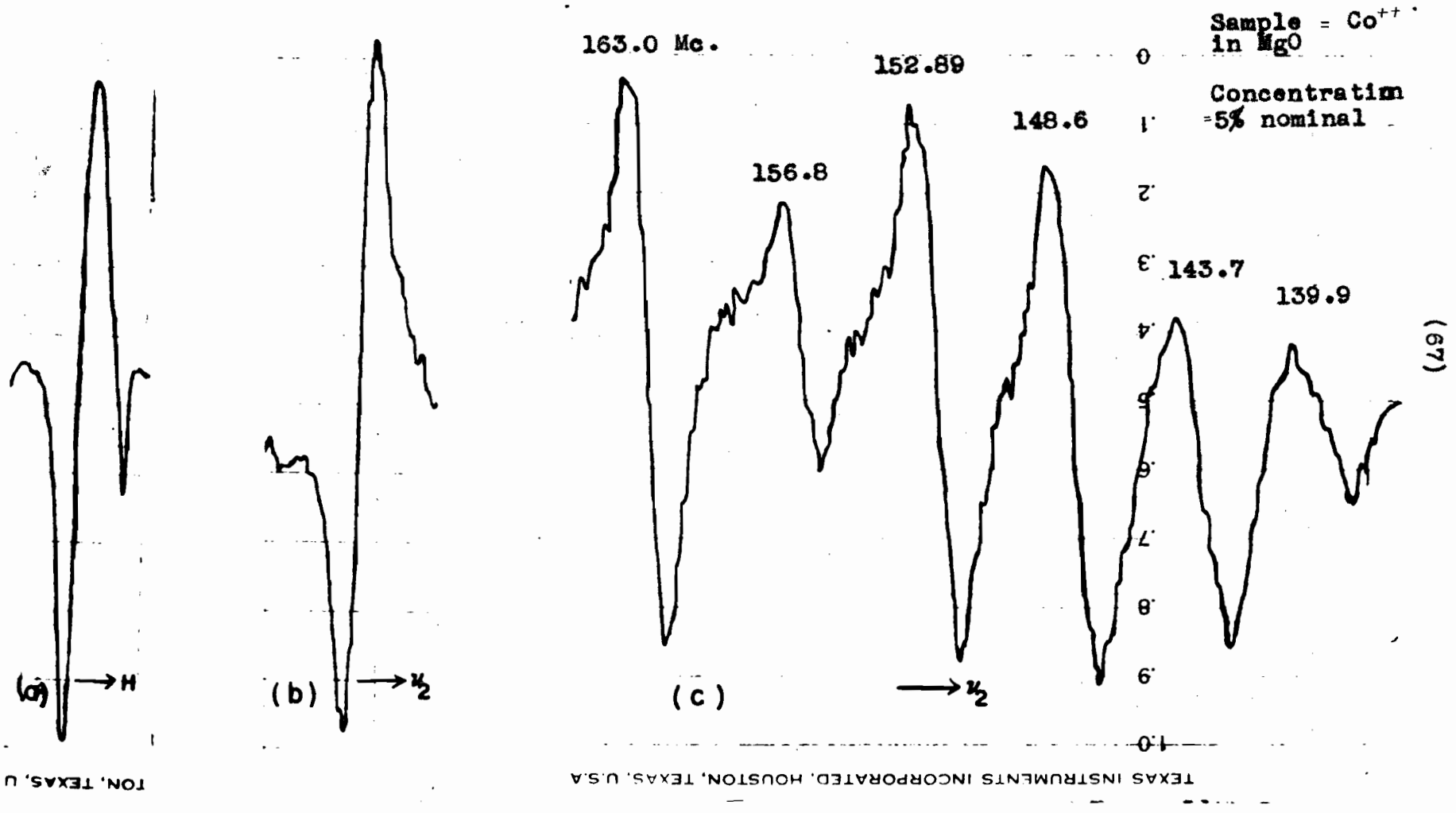

Fig. 11. Trace of the chart-recorder showing (a) the first high field EPR line (b) one of the two expected ENDOR transitions, (c) experimentally observed ENODR transitions. Phase in (c) is opposite to that of (b) because the bridge was again balanced.

well-suited for checking the effect, on the signal, of varying the amount of modulation. The same measurements could be done by using external modulation at any frequency (up to 25 Kc/s), either F.M. or A.M.

In the range of frequency (120 to 240 Mc/s) used for the following experiments the frequency deviation could be varied up to a maximum of slightly over 600 Kc/s. With the intention of getting as many readings as conveniently possible, the frequency deviation was varied in steps of 40 Kc/s and a trace of the double resonance line was taken for each step. The graph of ENDOR signal as a function of modulation index, defined by

$$\text{Modulation index} = \frac{\text{Frequency Deviation}}{\text{Modulating frequency}}$$

was found to be having two straight line parts which have different slope, and which cannot join in a reasonable manner.

The experiment was repeated several times and a similar type of graph, as shown in the graph 4, was obtained indicating that either the bridge is thrown off balance, or the cavity has gone off-tune, or both. To reduce the effect of these troubles it was decided to take only a few readings in a short interval of time so that the effects of the above mentioned difficulties are reduced. It was then observed that the double resonance signal varied directly with the modulation index as shown by the graph 5. These graphs show that very great care should be taken to avoid disturbing the balanced

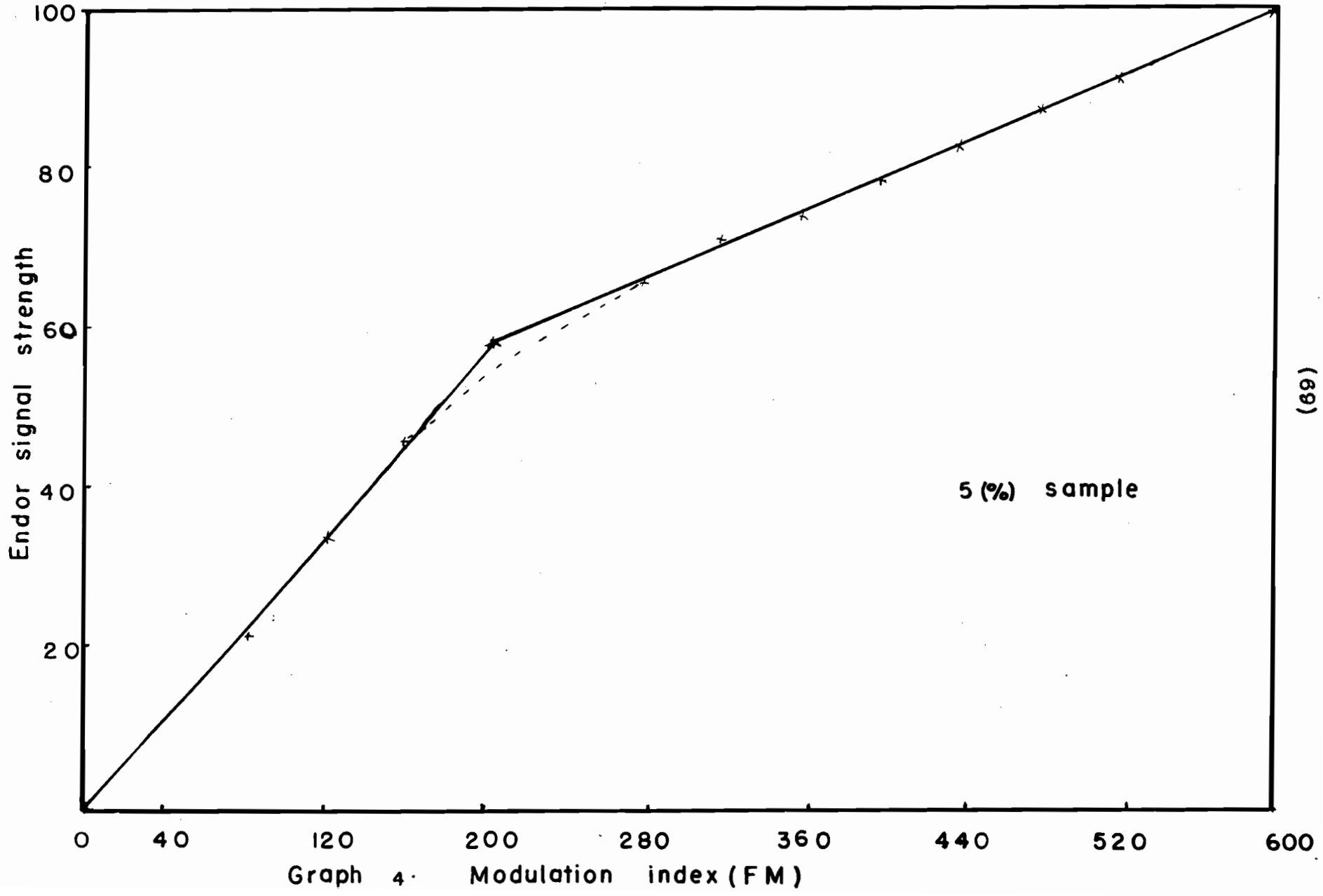
100
80
60
40
20
Endor signal strength
5 (%) sample
0
40
120
200
280
360
440
520
600
Modulation index (FM)

Graph 4.

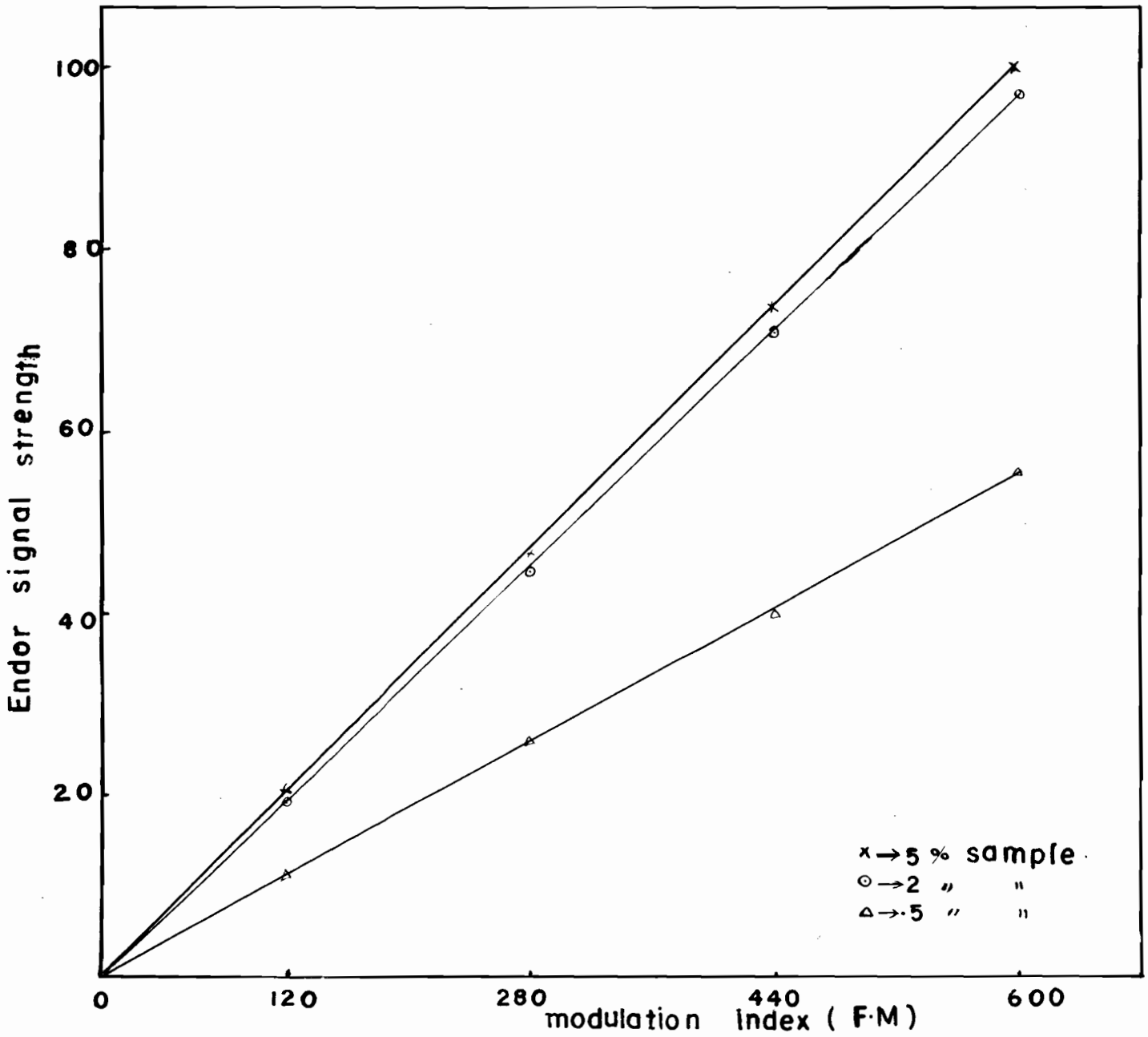
100
80
60
40
20
Endor signal strength
0
120
280
440
600
modulation index (F·M)
× → 5 % sample
⊙ → 2 " "
△ → ·5 " "

Graph 5.

bridge and detuning the cavity which may arise even by accidental touching of the table supporting the devar and wave-guide assembly.

This method of measurement was repeated for all the three samples and it was found, in each case, that the signal strength is directly proportional to the modulation index and also to the concentration of the paramagnetic sample.

(4) Dependence of Double Resonance Signal with % A.M.:-

The amplitude modulation does not produce any drastic improvement in signal strength over F.M. Measurements were however undertaken to study the relative strengths of signals obtained by this method and those obtained by F.M. The percentage A.M. could be varied from zero up to a maximum of 80%. The strength of double resonance signal was measured between these limits. It was found that it is directly proportional to the percentage amplitude modulation as shown by the graph 6, for each concentration.

It is worth noting that this set of measurements was intended as a quick confirmation of the linearity of signal increase with the amount of modulation, which appears almost certain from the way the equipment is set up. Instead, however, the measurements caused considerable trouble, and since the early peculiar results appeared consistent, a certain amount of

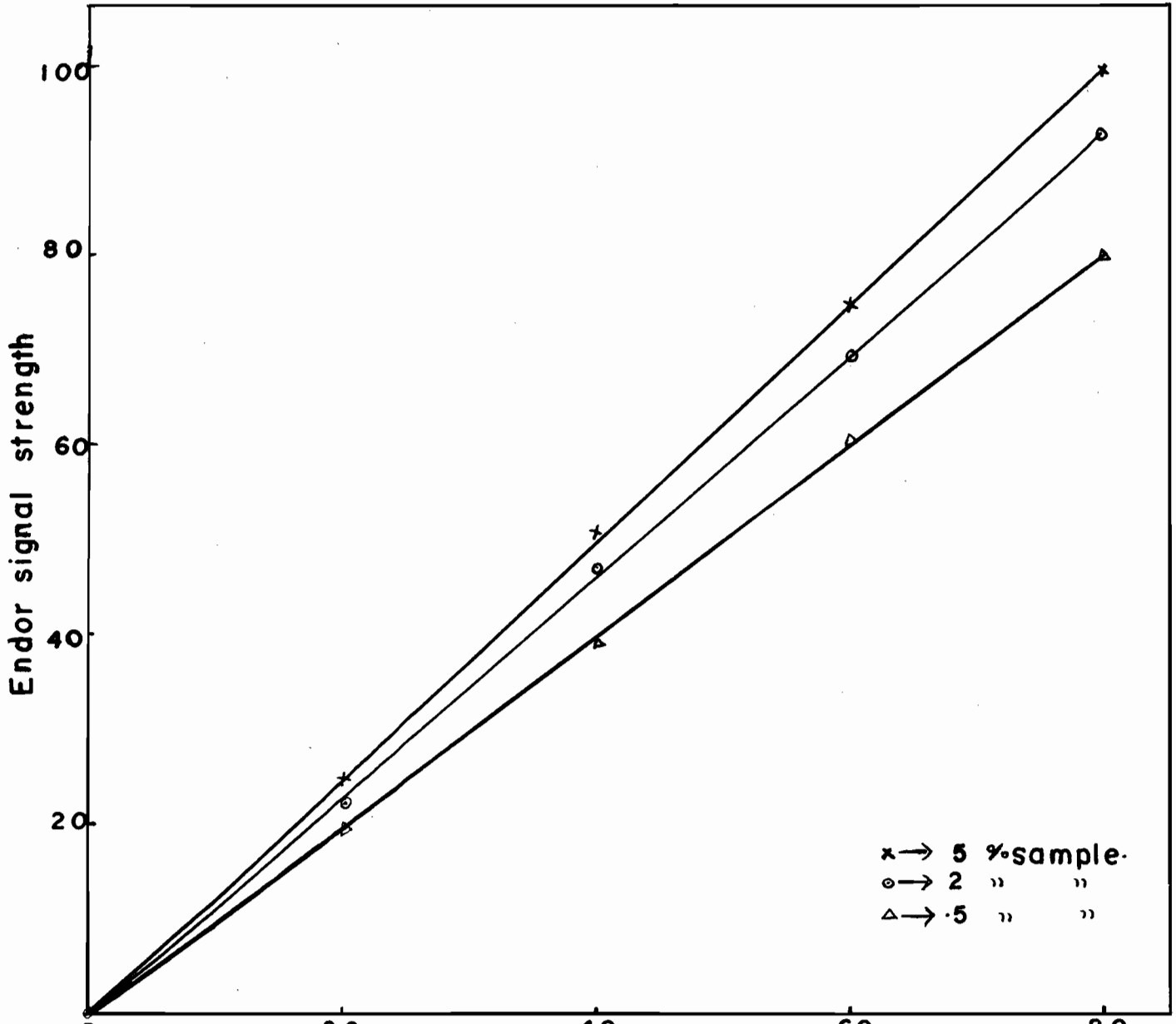
100
80
60
40
20
0
20
40
60
80
Endor signal strength
Percentage modulation (A·M)
x → 5 % sample·
⊙ → 2 " "
△ → ·5 " "

Graph 6·

time was spent trying to explain these results. Eventually it became evident that the bridge drifted off-balance very rapidly at times, so the measurements were repeated, taking particular care to do a series in as rapid succession as possible. This method gave the expected linear dependence. It is obvious however that steps must be taken to prevent this trouble by some change in design of the equipment. The source of the drift is however not yet very clear. It is possible that it might be due to the frequency variations of the local oscillator.

Comparison of F.M. and A.M.:-

A qualitative comparison of the ENDOR signal obtained by F.M. and A.M. may now be given in brief. The main difference between the signals obtained by the two different methods is in the shape of the lines. The derivative of the absorption signal () was observed with F.M. while the absorption signal () itself was obtained with A.M. Even though the signal strength varies linearly with the F.M. deviation in the case of frequency modulation and with percentage A.M. in the case of amplitude modulation it was found, with maximum F.M. and A.M, that the signal is always stronger with the former than with the latter. F.M. will always eventually distort the line-shape as it is increased, and a reasonable limit in the present case is 200 Kc/s. This limit may be small for narrow lines. A.M. however is a constant frequency, not a sweeping of frequency, and so should not introduce any distortion even at 80% A.M.

At lower modulation levels the signal to noise ratio is poor until it becomes very hard to tell which is better ofthe two, at very small amounts of modulation.

(5) Variation of ENDOR Signal with Second Frequency (γ_2) Voltage:-

The amount of second frequency power is determined by the maximum voltage of signal generator, maximum gain of wide-band amplifiers and maximum power output of wide-band amplifiers. The wide-band amplifiers following are used at maximum gain; one of them has in fact fixed gain. This output power is controlled by attenuators in the signal generator which indicate the output voltage when the meter reading (cw) is set to the 0 db mark, are calibrated in μv and db/μv across 50 or 75 ohms, and can be set to values from 100 mv (100 db) down to 0.1 μv (-20 db). But no double resonance signal was observed when the attenuator setting was 80 db (corresponding to 10,000 μv) and below. Hence this was taken as zero and from this zero, power was increased in steps of 4 db up to 20 db maximum. This was amplified by the two wide-band amplifiers before feeding into the ENDOR coil. The output from these wide-band amplifiers varies approximately from 1 volt to 6 volts corresponding to these settings. For each of these values of the γ_2 voltage the peak-to-peak value of the ENDOR signal was measured. A graph is drawn by plotting the second frequency voltage against the intensity of the signal. Several

sets of readings were taken for each of the three samples used. It was found, for each sample, that the strength of the signal changes linearly with the γ_2-voltage as shown by the graph 7. These graphs do not pass through the origin. This may be due to the fact that there is a certain amount of threshold voltage below which no ENDOR signal is possible. Points on the graph corresponding to maximum available γ_2-voltage do not lie on the line for reasons which are not clear though the result is reproducible. It may be possible to investigate this if we had another wide-band amplifier and this would be done as soon as one is available.

(6) <u>To investigate the dependence of the strength of the Double Resonance Signal on Spin Temperature:-</u>

While discussing the conditions for a good double resonance signal it was shown, for the case where the rectified power is proportional to the incident power (linear region), that the spin temperature T_s should be doubled for getting a good ENDOR signal, as given by the expression,

$$\frac{T_s}{T_B} = \frac{n_o}{n_s} = 1 + \gamma^2 H_1^2 \; T_1 \; T_2 \simeq 2$$

where all the quantities are as defined before.

The following experiments were done with the intention of studying the dependence of the ENDOR signal on the spin temperature. The method of approach is as follows.

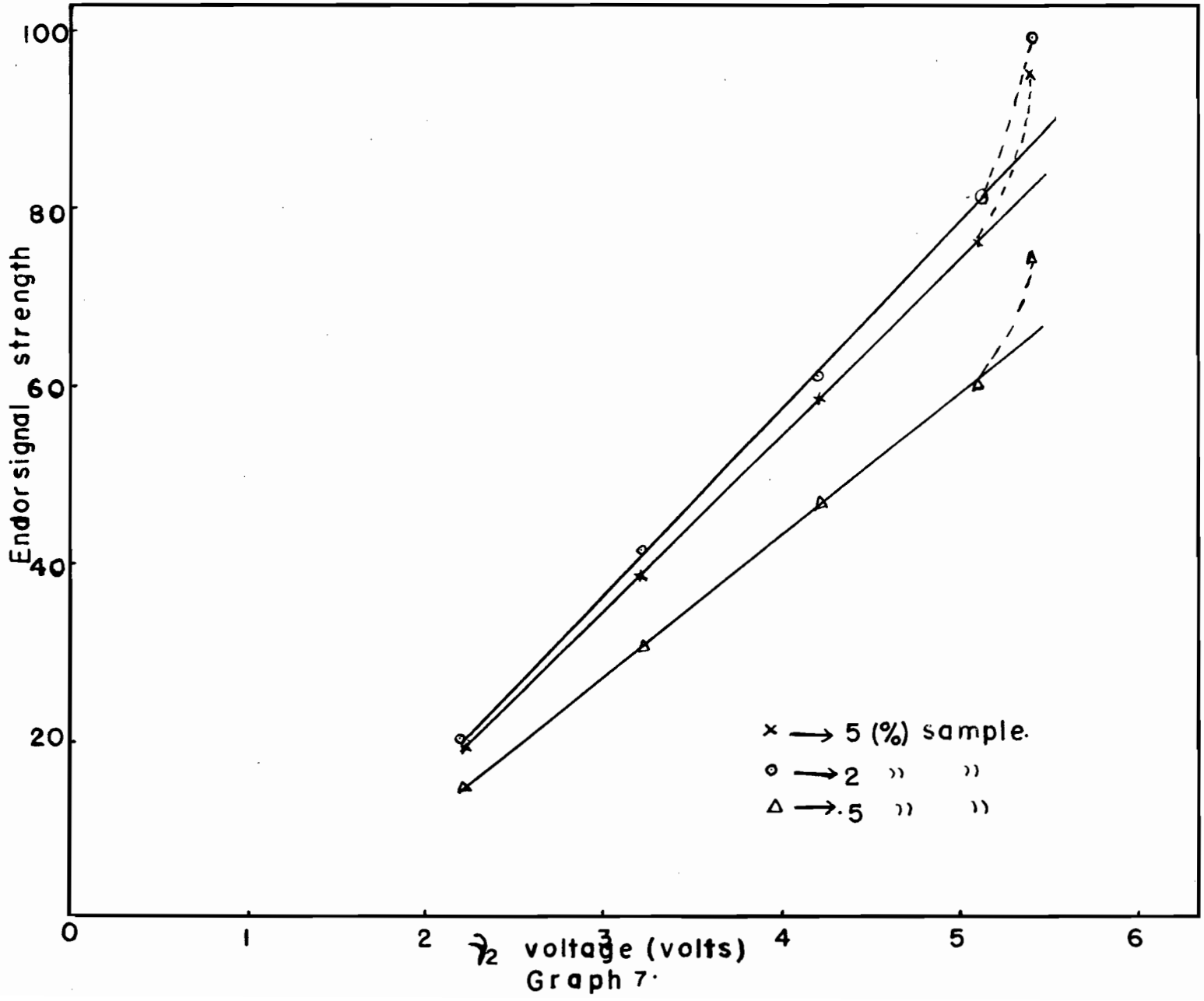
100
80
60
40
20
Endor signal strength
0
1
2
3
4
5
6
γ_2 voltage (volts)
× → 5 (%) sample.
○ → 2 " "
△ → .5 " "

Graph 7.

The combinations of A_1 and A_2 were found experimentally which gave the best double resonance signal for each sample used. The spin temperature is now varied by varying the power incident on the sample in either direction, but keeping the amount of power incident into the receiver system always constant, and a trace of the signal is obtained. This is repeated in steps of a few decibels on either side of the optimum setting and the strength of the signal is measured in each case. A typical graph drawn with the signal along the ordinate and the amount of power incident on the sample (which is proportional to the spin temperature) along the abscissa is shown in the graph 8.

This graph is for the low concentration sample. It is clear from the graph that the strength of the signal decreases on both sides of the optimum value. It also shows that the signal falls rather rapidly if the spin temperature is less than the optimum while the fall is a little less rapid if the spin temperature is larger than the optimum.

The general nature of the curves for the other samples is quite similar to the one discussed above though the optimum attenuator setting i.e., input power, is different for different concentrations as shown by the dotted curves on page 78.

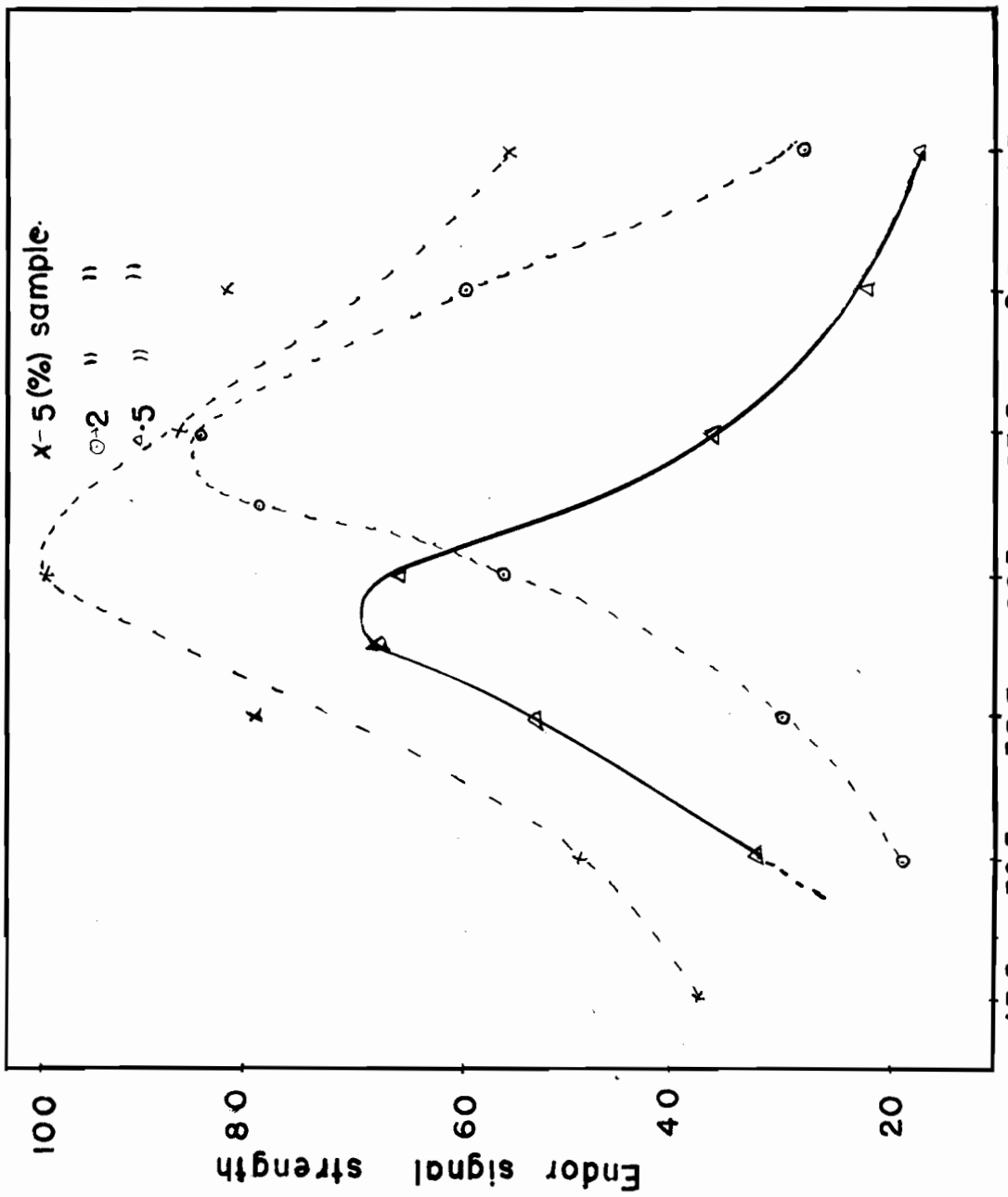
X-5 (%) sample.
⊙ 2 " "
• 0.5 " "
Endor signal strength
100
80
60
40
20
43.5
38.5
33.5
28.5
23.5
18.5
13.5
Microwave power (db. below 1 watt)

Graph 8.

CONCLUSION

The optimum working conditions of ENDOR spectrometer has been found out for each of the three MgO samples containing Co^{++} ions. Graph 1 for the 5% sample indicates that the spin temperature of the EPR line corresponding to the transition $M_S = \frac{1}{2} \longleftrightarrow \frac{-1}{2}$ and $m_I = \frac{-7}{2} \longleftrightarrow \frac{-7}{2}$ is doubled when the power incident into the cavity is 24 db. below 1 watt. Referring to the table on page 62 shows that the corresponding setting A_1 is 10 db. If we add 13.5 db. to this value (converting the power incident on the sample into decibels below 1 watt and taking into account the attenuation due to the wave-guide assembly) we see that the best ENDOR signal could be obtained when the power incident was 23.5 db. below 1 watt, in close agreement with that indicated by the graph.

From graph 2 for the 2% sample and for the same transition 26 db. below 1 watt corresponds to the doubling of the spin temperature. The table shows that the best ENDOR signal is obtained when the power incident is 26 db. below 1 watt, again in close agreement.

The same is true for the 0.5% sample as shown by the graph 3 and the table.

The dependence of the ENDOR signal with the amount of F.M. and A.M. is quite straight forward and linear as expected as shown from the graphs 5 and 6 respectively. The main difference between the ENDOR signal obtained by F.M. and that by A.M. is in the line shape. Also, at high modulation F.M. distorts the line, a deviation of about 200 Kc/s being the limit for samples of higher concentrations, while A.M. does not distort the ENDOR line for reasons mentioned before.

The EPR and ENDOR signals decay with time. This is due to progressive imbalance of the bridge, the main question being what causes this imbalance. This may be due to the fact that the electrical length of the wave-guide leading to the cavity changes due to the boiling away of liquid helium as a result of which there is a change in phase. A simple calculation showed that this produces a few degrees change of phase. This may cause the microwave bridge to go off-balance which is responsible for the decaying signal. However, this effect should be small when compared to the others which may be responsible for this trouble. Another possible source causing this effect may be the local oscillator whose frequency fluctuations may be large in comparison with the band-width of the pre-amplifier. This could be avoided by using another stabilized klystron in place of the local oscillator. For further work it is intended to use either a stabilized local oscillator

or to get the 30 Mc/s beat from the main klystron itself by a modulation system.

Dependence of the ENDOR signal on γ_2 - voltage is found to be linear as expected, but the graph of ENDOR signal plotted against γ_2 - voltage does not pass through the origin. The point on the graph corresponding to the maximum available γ_2 - voltage does not lie on the straight line. Insufficient γ_2 - voltage is available to extend the range of measurements, without which one cannot say how genuine the rise is. At the moment, the highest points seem however quite genuine and reproducible. Obviously further investigation is needed when the available power can be increased by using another wide-band amplifier.

Graph 8 shows that the amplitude of the ENDOR signal falls as the microwave power incident on the sample is either increased or decreased from the optimum value. Though the general nature of the curves is the same for different concentrations of the sample, the optimum value is different for each.

The dependence of the ENDOR signal on the direction of the D. C. magnetic field is useful and interesting. It is intended to make further studies on this as soon as the equipment for the finer magnet control, which is being designed and built, is ready.

It is also proposed to undertake the ENDOR line-width measurements as soon as some improvements on the accuracy of measuring frequencies are made.

The measurements made in this project seem to be quite straight forward. This is only true provided the equipment functions properly without any drift caused by the detuning of the cavity and frequency fluctuations. But, for the type of work done in this course, it is very hard and time consuming to get consistent results unless great precautions are taken. These measurements may help in further understanding the double resonance theory.

APPENDIX

EXPERIMENTAL PROCEDURE FOR ENDOR

Getting the trace of a double resonance signal involves various routine steps which are outlined below. It is assumed that the reader is familiar with the major adjustments, such as stabilizing the main klystron etc. As EPR is pre-requisite of ENDOR, the experimental procedure of the former is also dealt with in brief.

To start with the sample is positioned in the ENDOR coil in the appropriate orientation and the coil is inserted into the cavity. The following routine procedure is followed at liquid helium temperature.

(1) The cavity is tuned for resonance.

(2) The local oscillator klystron is tuned until the meters registering the crystal current and the V.T.V.M. show maximum readings. The reflector voltage of the main klystron should also be adjusted by the fine control to achieve this.

(3) The attenuator and the phase control in the dummy arm of the magic - T are adjusted in turn until the reading on the V.T.V.M. is a minimum. After achieving this the attenuator control is slightly turned to make the output of the magic - T proportional to the derivative of the absorption signal only.

(4) With the switch controlling the modulation of the steady field on, and 200 c/s signal connected to the reference input of the P.S.D., the attenuators A_1 and A_2 are set in such a way that the I.F. amplifier is not saturated. A trace of the EPR signal is obtained on the recorder and its amplitude measured. Increasing the power incident on the sample by a few decibels at a time but keeping the power input to the receiver constant, the amplitufe of the trace of the EPR signal is measured in each case. The amount of power incident on the sample is calculated by knowing the reading of the power meter and the typical saturation curves shown in graphs 1, 2 and 3 are drawn. The frequency of the main klystron at which the signal appears can be measured by means of a cavity frequency-meter. If a measure of the D.C. field is also required it can be obtained by N.M.R. apparatus.

For getting an ENDOR signal the following routine is followed in addition to that explained above.

(5) The slow sweep of the steady magnetic field is stopped when the pen of the recorder is exactly at the centre of the derivative of the EPR signal.

(6) 1000 c/s reference to the p.s.d. is connected instead of 200 c/s during EPR.

(7) Because the internal modulation of the second frequency is sufficient the switch controlling the modulation of the steady field is switched off.

(8) The band-width of the band-pass filter is adjusted so that it passes only a few cycles around the frequency of 1000 c/s.

(9) The cavity is tuned and the microwave bridge is again balanced.

(10) The second frequency is swept slowly by means of a clock-motor until double resonance signals appear on the chart-recorder at the appropriate frequencies which may be measured by means of a frequency counter.

(11) Once the ENDOR signal is obtained, its dependence on microwave power, amounts of frequency and amplitude modulation and on the second frequency voltage can be measured as described before and graphs drawn to explain their influence on the signal.

BIBLIOGRAPHY

1. G. Feher, Physical Review 103, 500 (1956).

2. B. Bleaney and K.W.H. Stevens, Reports on Progress in Physics, Vol. XVI, (1951).

3. K.D.Bowers and J. Owen, Reports on Progress in Physics Vol. XVIII, (1955).

4. E.R.Andrew, Nuclear Magnetic Resonance - Cambridge Monographs on Physics, (1958).

5. J.H. Van Vleck, Electric and Magnetic Susceptibilities, Oxford University Press, (1932).

6. D.J.I.Fry, Ph.D. Thesis, 1961.

7. W.Low, Paramagnetic Resonance in Solids, Solid State Physics, Supplement 2.

8. Abragam and M.H.L.Pryce, Proc. Roy. Soc. of London A 205, 135, (1951).

9. M.H.L. Pryce, Physical Review 80, 1107 (1950)

10. M.H.L.Pryce, Proceedings of Physical Society A 63, 25 (1950).

11. Abragam and M.H.L.Pryce, Proc. Roy. Soc. A 206, 173, (1951).

12. W.Low, Physical Review 109, 247 (1958).

13. Condon and Shortley, Theory of Atomic Spectra Cambridge.

14. G. Feher, Physical Review 103, 834 (1956).

15. G. Feher, The Bell System Technical Journal Vol. XXXVI, No. 2, March 1957.

16. R.V.Pound, Technique of Microwave Measurements, Vol.II Radiation Laboratory Series, Chapter 2.

17. R.W.Terhune, J. Lambe, C.Kikuchi and J.Baker, Physical Review, Volume 123, 1265 (1961).